© 2022. Published by The Company of Biologists Ltd | Journal of Experimental Biology (2022) 225, jeb244474. doi:10.1242/jeb.244474

RESEARCH ARTICLE

The role of carbonic anhydrase-mediated tissue oxygen extraction in a marine teleost acclimated to hypoxia

Angelina M. Dichiera[1,*], Benjamin Negrete, Jr[2], Kerri Lynn Ackerly[2] and Andrew J. Esbaugh[2]

ABSTRACT

With the growing prevalence of hypoxia (O_2 levels $\leq$2 mg l^{-1}) in aquatic and marine ecosystems, there is increasing interest in the adaptive mechanisms fish may employ to better their performance in stressful environments. Here, we investigated the contribution of a proposed strategy for enhancing tissue O_2 extraction – plasma-accessible carbonic anhydrase (CA-IV) – under hypoxia in a species of estuarine fish (red drum, *Sciaenops ocellatus*) that thrives in fluctuating habitats. We predicted that hypoxia-acclimated fish would increase the prevalence of CA-IV in aerobically demanding tissues to confer more efficient tissue O_2 extraction. Furthermore, we predicted the phenotypic changes to tissue O_2 extraction that occur with hypoxia acclimation may improve respiratory and swim performance under 100% O_2 conditions (i.e. normoxia) when compared with performance in fish that have not been acclimated to hypoxia. Interestingly, there were no significant differences in relative CA-IV mRNA expression, protein abundance or enzyme activity between the two treatments, suggesting CA-IV function is maintained under hypoxia. Likewise, respiratory performance of hypoxia-acclimated fish was similar to that of control fish when tested in normoxia. Critical swim speed (U_{crit}) was significantly higher in hypoxia-acclimated fish but translated to marginal ecological benefits with an increase of ∼0.3 body lengths per second. Instead, hypoxia-acclimated fish may have relied more heavily on anaerobic metabolism during their swim trials, utilizing burst swimming 1.5 times longer than control fish. While the maintenance of CA-IV may still be an important contributor for hypoxia tolerance, our evidence suggests hypoxia-acclimated red drum are using other mechanisms to cope in an O_2-depleted environment.

KEY WORDS: Phenotypic plasticity, Respiratory gas exchange, Low oxygen, Metabolic rate, Swim performance

INTRODUCTION

The solubility of O_2 in open and coastal oceans is decreasing at an alarming rate (Bopp et al., 2013; Ito et al., 2017), exacerbated by the concurrent rise in sea-surface temperatures. In coastal regions, anthropogenic activities also contribute to reduced O_2 availability (e.g. eutrophication; reviewed by Diaz and Rosenberg, 2008), increasing the prevalence and range of habitats experiencing O_2 levels $\leq$2 mg l^{-1} (i.e. hypoxia; Rabalais et al., 2010, 2002). While some fishes can move from unfavorable habitats, there are limitations when hypoxic episodes are increasing both spatially and temporally. As such, the ability to survive and perform in hypoxic conditions is incredibly important for most aquatic organisms, and has even recently been hypothesized to contribute to marine species' equatorial distributions (Deutsch et al., 2015, 2020).

With the sheer diversity of fish species, our knowledge of the adaptive strategies and flexible mechanisms fish employ in hypoxia is continually expanding. Generally, fish exposed to reduced environmental O_2 try to maintain metabolic rate (e.g. Fry, 1947; Negrete and Esbaugh, 2019) to preserve routine O_2 delivery to aerobically demanding tissue (e.g. heart and brain). Metabolic demand in fish can be defined by the Fick equation:

$$\dot{M}_{O_2} = \dot{Q} \times (Ca_{O_2} - Cv_{O_2}), \quad (1)$$

where $\dot{M}_{O_2}$ is metabolic rate, $\dot{Q}$ is cardiac power (i.e. heart rate and stroke volume) and Ca_{O_2}–Cv_{O_2} is the difference between arterial and venous O_2 content (i.e. tissue O_2 extraction). Under hypoxia, many fish prioritize reduced cardiac O_2 demand via decreased heart rate (bradycardia; reviewed by Farrell, 2007) and overall reduced cardiac power (reviewed by Esbaugh et al., 2021). Conversely, to compensate for reduced total blood O_2 content under hypoxia due to limitations in environmental O_2, fish can employ mechanisms to improve O_2 uptake and tissue O_2 extraction, such as hyperventilation (e.g. Ern and Esbaugh, 2016) and changes to blood O_2 binding characteristics (e.g. Fu et al., 2011; Mandic et al., 2009; Pan et al., 2017).

While O_2 diffusion at both the gill and tissue is a passive process driven by O_2 partial pressure (P_{O_2}) gradients, some species demonstrate active processes that can increase P_{O_2} gradients and enhance tissue O_2 extraction (recently reviewed by Harter and Brauner, 2020). Many teleost fish possess Root effect hemoglobins (Hbs), which have an extreme sensitivity to pH (Pelster and Weber, 1991; Root, 1931). Even at high P_{O_2} levels, a decrease in pH will decrease the capacity of Hb to bind O_2. Originally, this mechanism was thought to be beneficial for areas of localized acidosis to help offload O_2 to demanding tissues, such as the eye (choroid rete) and swim bladder (rete mirabile; Berenbrink et al., 2005). Rummer et al. (2013) later proposed that Root effect Hb may also have benefits for other aerobically demanding tissues such as the red muscle. During bouts of stress (e.g. exercise, hypercapnia, hypoxia), β-adrenergic sodium proton exchangers (βNHE) in the red blood cell (RBC) are activated by catecholamines to protect intracellular pH and Hb–O_2 binding affinity by extruding protons (H^+). This helps maintain RBC O_2 loading at the gill (Nikinmaa, 1982; Nikinmaa et al., 1990; Salama and Nikinmaa, 1988). At the red muscle, plasma-accessible carbonic anhydrase (paCA or CA-IV) short-circuits this protection mechanism by producing additional CO_2, increasing RBC acidification, thereby overwhelming βNHE and consequently

[1]Department of Zoology, The University of British Columbia, Vancouver, BC, Canada V6T 1Z4. [2]Marine Science Institute, The University of Texas at Austin, Port Aransas, TX 78373, USA.

*Author for correspondence (dichiera@zoology.ubc.ca)

A.M.D., 0000-0002-9635-0229; B.N., 0000-0001-6030-6122; K.L.A., 0000-0002-3111-724X; A.J.E., 0000-0002-7262-4408

Received 28 April 2022; Accepted 12 October 2022

Journal of Experimental Biology (2022) 225, jeb244474. doi:10.1242/jeb.244474

increasing O_2 offloading from Hbs to the muscle (Rummer and Brauner, 2011, 2015; Rummer et al., 2013). The process of βNHE short-circuiting via CA-IV has also been investigated in the heart and eye (Alderman et al., 2016; Damsgaard et al., 2020). Species with active lifestyles or that regularly encounter environmental stress may therefore benefit from increased abundance of CA-IV to help drive O_2 offloading to a range of aerobically demanding tissues.

Red drum (*Sciaenops ocellatus*) are an estuarine species known to thrive in habitats that frequently fluctuate in salinity, temperature, CO_2 and O_2, and as such display a flexible phenotype to a number of environmental stressors (Allmon and Esbaugh, 2017; Ern and Esbaugh, 2016; Esbaugh and Cutler, 2016; Lonthair et al., 2020, 2017; Martin and Esbaugh, 2021; Pan et al., 2016, 2017; Watson et al., 2014). CA-IV is present in the red muscle and heart of this species (Dichiera and Esbaugh, 2020), but its dynamic regulation in these tissues following environmental stress is unknown. For fish such as red drum that regularly encounter low O_2 in the coastal regions of the Gulf of Mexico, respiratory plasticity may provide a path to increased O_2 uptake and extraction leading to elevated respiratory performance under hypoxia. Previous work in our lab has demonstrated that in response to prolonged hypoxia exposure, red drum alter transcriptional regulation of Hb isoforms, which is correlated with increased Hb–O_2 binding affinity, and a reduced critical O_2 threshold (P_{crit}; Pan et al., 2017) and improved maximum metabolic rate (MMR) when tested in hypoxia (Negrete et al., 2022). Here, we assessed the role of CA-IV in hypoxia-induced respiratory plasticity, which had been suggested by Harter et al. (2019) as a mechanism fish may employ to increase tissue O_2 extraction. Specifically, we utilized a 6 week chronic hypoxia-acclimation protocol to assess the plasticity of tissue O_2 extraction via dynamic transcriptional regulation of CA-IV in the heart and red muscle, as well as NHE1 and RBC CA, which has recently been implicated in tissue O_2 extraction mechanisms in red drum (Dichiera and Esbaugh, 2020). We then performed follow-up analysis to validate transcriptional signals at the protein level, and a critical swim speed (U_{crit}) protocol to assess potential improvements in O_2 transport capacity and whole-animal respiratory performance.

MATERIALS AND METHODS

Animal care and handling

Red drum, *Sciaenops ocellatus* (Linnaeus 1766), were purchased from Ekstrom Aquaculture LLC (El Campo, TX, USA) and held at the Fisheries and Mariculture Laboratory at The University of Texas at Austin Marine Science Institute (Port Aransas, TX, USA). Fish were fed *ad libitum* except for the 48 h prior to sampling. All experimental protocols were approved by the University of Texas at Austin Institutional Animal Care and Use Committee (AUP-2018-00231).

Series I: gene expression, protein abundance and localization

Hypoxia acclimation and tissue sampling

The experiment described here was performed in tandem with the work of Negrete et al. (2022), which focused on Hb plasticity during hypoxia acclimation. Fish were held in ∼250 l recirculating tanks (25 ppt; 24.7±0.03°C). Briefly, juvenile red drum were chronically exposed to either normoxia (n=33, mean±s.e.m. mass: 64.8±2.7 g, dissolved O_2, DO: 100.0±0.1%, pH: 8.02±0.01) or hypoxia (n=35, mass: 61.9±2.0 g, DO: 33.3±0.2%, pH: 8.10±0.01). Hypoxia was regulated via bubbled nitrogen using automated Oxy-Reg systems (Loligo® Systems). All tanks were partially covered with bubble wrap to prevent O_2 surface mixing. Fish were divided among three replicate tanks for each treatment, with 2–3 fish terminally sampled from each tank at 1 day, 4 days, 8 days, 2 weeks and 6 weeks (n=6–8 per treatment per time point). Prior to sampling, fish were moved to isolated boxes in their acclimation water where an overdose of MS-222 (250 mg l^{-1} buffered with 500 mg l^{-1} $NaHCO_3$) was introduced to prevent any handling stress, followed by spinal transection. Red muscle and ventricle samples were collected and partitioned to assess gene expression, protein abundance and immunohistochemistry of CA-IV. To address additional components of the tissue O_2 extraction pathway, blood was collected for gene expression of *nhe1* and *rbc ca*. Blood was sampled via caudal puncture and centrifuged for 2 min at 10,000 ***g*** to separate RBCs from plasma. Plasma was discarded and RBCs were washed thrice with isotonic saline (300 mOsm l^{-1} NaCl) to remove any remaining plasma or extracellular components. For gene expression and protein abundance, tissues were stored at −80°C until use. For immunohistochemistry, samples were placed into Z-fix commercial fixative solution overnight, and then transferred to 70% ethanol until use.

mRNA expression

Red muscle and ventricle tissue samples were processed for total mRNA using TriReagent (Molecular Research Center, Inc.), in accordance with manufacturer protocols. RBC samples were processed using the GeneJET RNA purification kit (Thermo Scientific). All mRNA was quantified using an ND-1000 spectrophotometer (Thermo Scientific). To treat for potential DNA contamination, mRNA underwent DNase I treatment (1 U μl^{-1}) prior to cDNA synthesis (Invitrogen). First-strand cDNA was synthesized using 1 µg (heart and red muscle) or 0.5 µg (RBC) of total RNA and RevertAid reverse transcriptase (Thermo Scientific). Controls with no reverse transcriptase (no-RT) were included with each batch of cDNA samples, and all samples were diluted 10-fold with nuclease-free water and stored at −20°C until qPCR analysis.

qPCR analysis was performed using Maxima SYBR green/ROX qPCR Master Mix (Thermo Scientific). Primer pairs used here for red drum can be found in Table 1, and have previously been published and validated (Dichiera and Esbaugh, 2020). Standard curves were developed for each primer pair using a 2-fold dilution series of cDNA. Negative (nuclease-free water) and no-RT control reactions were performed with all genes. All relative expression values were calculated relative to 1 day normoxia and normalized using *ef1α*. All calculations were performed according to the modified ΔΔCt method (Pfaffl, 2001).

CA-IV protein quantification

Two primary rabbit CA-IV antibodies were custom made against distinct regions of the protein (GenScript®) and both were validated using control and hypoxia heart samples from 4 days using Western blots (Fig. S1). A primary antibody concentration of 1:1000 in blocking buffer [5% skim milk powder in Tris-buffered saline with 1% Tween (TBST)] was successfully tested against 10 µg heart protein and 30 µg red muscle protein (linear response validation can be found in Fig. S2). One of the two antibodies was then used for protein quantification. Membrane-bound protein was isolated from control and hypoxia heart and red muscle samples at 8 days using 1 ml RIPA buffer (Amresco®) per 40 mg tissue and processing according to manufacturer protocols. Briefly, tissue was sonicated for 30 s, shaken gently for 15 min on ice, centrifuged at 14,000 ***g*** for 15 min, and the supernatant (isolated protein) was removed. Protein

Journal of Experimental Biology (2022) 225, jeb244474. doi:10.1242/jeb.244474

Table 1. Primers used for qPCR

Gene	Accession no.	Orientation	Primer
ef1α	KJ958539	F	GTCCGTACATGAGGCAGACTG
		R	GTTGCTGGATGTCCTGCACG
ca4	MT362925	F	GCAGTCCTTGGGTTTTTCTATG
		R	TGGTCATATTCTGCTCAGATGG
rbc ca	KM387715	F	TCAACATCGTCCCCAAGGAGG
		R	ATAGGACCTCCAGTCAGGGTGG
nhe1	KU899107	F	AATGAGCTGCRGCACATCCTCG
		R	CAGACCACTCCGAGGACAGC

All sequences are 5′ to 3′ and reverse primers are complements of the genetic sequence.

was quantified using a bicinchoninic acid protein assay (G-Biosciences®) using albumin standards (Thermo Scientific). Western blot protocols were modified from procedures previously described for our lab (Esbaugh and Cutler, 2016). SDS-PAGE was performed using the Bio-Rad® Mini-PROTEAN electrophoresis system; 10 µg heart protein or 30 µg red muscle protein was loaded onto precast Mini-PROTEAN TGX stain-free gels (BioRad®) and separation was performed in an ice bath at 50 V for 5 min and 150 V for approximately 1 h. Chemi-doc MP imaging system (BioRad®) was used to activate the gel after SDS-PAGE, and protein was transferred from the gel to PVDF membrane using the Trans-Blot Turbo transfer system (BioRad®) according to manufacturer guidelines. Images were taken post-transfer of both the gel (to ensure successful transfer) and blot for total protein quantification, as described below. For CA-IV detection, each blot was: (1) rinsed with TBST and blocked for 1 h with blocking buffer; (2) rinsed with TBST 5 times for 5 min each; (3) incubated with 1:1000 CA-IV primary antibody overnight at 4°C; (4) rinsed with TBST 5 times for 5 min each; (5) incubated with 1:10,000 horse radish peroxidase (HRP) conjugated anti-rabbit secondary antibody for 1 h; (6) rinsed with TBST 5 times for 5 min each; (7) visualized using Clarity Western ECL substrate kit (BioRad®) and the Chemi-doc MP imaging system with autodetect chemiluminescent settings. The specificity of the antibody was validated using an antibody antigen pre-treatment protocol (10× antigen excess, overnight incubation at 4°C), which resulted in the disappearance of target bands (Fig. S3).

To quantify changes in CA-IV protein content across time and between treatments, a control heart sample from the 8 day time point was included on each gel for standardization purposes. Using the Chemi-doc MP imaging system, bands were detected, and quantities were assigned relative to the standard sample, both for total protein content of each sample (using stain-free SDS-PAGE blot images prior to antibody incubation) and for CA-IV protein content. Relative CA-IV protein content was divided by relative total protein content for each sample. We detected two bands using our CA-IV antibody (43 kDa and 56 kDa) in the heart sample, which we ascribe to the mature and immature protein, respectively. Note that as a GPI-linked protein, CA-IV undergoes post-translational modification prior to being incorporated into membranes. Our presumption was confirmed by preliminary validation tests using protein isolated using the commercially available Mem-PER™ Plus membrane protein extraction kit (Thermo Scientific) according to the manufacturer protocol, whereby the smaller band was detected in the membrane fraction and the larger band was detected in the cytoplasmic fraction (Fig. S1). Protein expression was quantified for the mature 43 kDa band for both red muscle and heart at 8 days, and for the immature 56 kDa band for the heart at 8 days (red muscle did not show a strong signal for the immature 56 kDa band to warrant quantification; see Fig. S4). However, for our purposes of quantifying active CA-IV, we focused on the mature form here, and immature CA-IV data can be found in Fig. S5.

CA-IV localization

Only ventricle samples were analyzed for CA-IV localization. Immunohistochemistry was performed as per Lonthair et al. (2020). Fixed tissue samples were removed from 70% ethanol and dehydrated in a series of alcohol washes (three washes of 95% ethanol for 1 h; three washes of 100% ethanol for 1 h; one wash with butanol for 1 h and a second wash overnight), cleared with two washes of xylene for 90 min, and prepped for imbedding with two Paraplast® washes at 58°C for 1 h each. Paraplast® was then used to set the samples at room temperature, and samples were sectioned at 10 µm with a microtome. Two sections of each sample were mounted onto Superfrost Plus slides (one for a no-primary antibody control, one for CA-IV staining), where they were rehydrated, deparaffinized, and soaked in deionized water until ready to stain. Hydrophobic barriers were drawn around each sample to ensure the no-primary antibody control was separated from the treated sample. Samples were washed with blocking buffer [phosphate-buffered saline and 1% Tween (PBST) with 5% fetal calf serum] twice for 5 min, followed by incubation with 1:1000 primary rabbit CA-IV antibody (GenScript®) at 4°C overnight. After primary antibody incubation, samples were washed with blocking buffer 3 times for 5 min, then incubated with 1:500 secondary antibody goat anti-rabbit Alexa Fluor® 647 (Abcam) in the dark for 1 h at room temperature. Samples were washed with blocking buffer 3 times for 5 min, stained with Sudan Black for 20 min to reduce autofluorescence, and rinsed with PBS for 10 min. Finally, some samples (n=1 for control treatment, n=2 for hypoxia treatment) were mounted with Permount™ mounting medium (Fisher Chemical™) to qualitatively assess CA-IV localization alone, and some (n=1 for control treatment, n=1 for hypoxia treatment) were mounted with VectaShield® HardSet™ with DAPI to assess CA-IV staining in relation to nuclei. All were stored in the dark at 4°C until imaged. Confocal microscopy was performed using a Nikon C2+ confocal microscope system with a Nikon Eclipse Ti-E inverted microscope. Fluorescent and differential interference contrast (DIC) images were acquired and processed using NIS-Element imaging software. Two to four images were taken from a few unique ventricles per treatment (n=2 for control treatment, n=3 for hypoxia treatment).

Statistical analyses

Analyses were performed using R Studio (version 4.0.2; http://www.R-project.org/). All data were assessed for normality and homogeneity of variance prior to analyses, and natural log transformed to meet test assumptions when necessary. Samples with no CT values (non-detects) were not included in the analyses. Where transformed data failed normality tests, outliers (n=3) were identified via normal Q–Q plot evaluation and excluded from the

rbc ca gene expression during analyses. There were no statistical differences between replicate tanks and all following tests were performed on individuals. To determine the effects of time and treatment on gene expression, we used Type III two-way ANOVA (α=0.05). Tukey *post hoc* analyses were carried out when an interaction effect was detected. Student's *t*-tests (α=0.05) were used to determine the effect of treatment on protein quantity at 8 days.

Series II: enzyme activity

Hypoxia acclimation and tissue sampling

Subadult red drum were used in series II as activity assays for membrane-bound CA-IV require a large quantity of tissue (often tissues are pooled; e.g. Esbaugh and Tufts, 2006). Fish were held in ∼600 l recirculating tanks (34 ppt; 23.9±0.1°C). Red drum were exposed to either chronic normoxia (n=12, mass: 768.3±61.5 g, DO: 98.0±0.3%, pH: 7.82±0.01) or hypoxia (n=12, mass: 670.6±46.9 g, DO: 34.5±0.5%, pH: 7.74±0.01) for 8 days as described in series I. Similarly, washed RBCs, red muscle and ventricle samples were collected and stored at −80°C until use.

RBC CA activity

RBC CA activity was measured using a modified ΔpH method (Henry, 1991; Henry et al., 1993) using an Orion 8102BN ROSS Combination pH electrode (Thermo Scientific) as per Dichiera and Esbaugh (2020). RBC samples were lysed using a 1:500 dilution in deionized water. For the enzyme reaction, a 10 µl aliquot of lysate was added to 5 ml buffer medium (225 mmol l^{-1} D-mannitol, 13 mmol l^{-1} Tris base, 75 mmol l^{-1} sucrose) held at 4°C, and 200 µl of CO_2-saturated distilled water (generated through constant bubbling of 5 psi CO_2 into deionized water held at 4°C) was injected into the buffer medium using a gas-tight Hamilton syringe. The reaction rate was measured over a pH change of 0.15 units. The uncatalyzed reaction rate (CO_2-saturated water only) was subtracted from this reaction rate to obtain the true catalyzed reaction rate. Additionally, the buffer capacity (µmol H^+ pH $unit^{-1}$) was determined prior to the catalyzed and uncatalyzed reactions and was used to convert the reaction rates from pH units min^{-1} to µmol H^+ min^{-1}. All reactions were performed in triplicate. CA activity was standardized by protein content (µmol H^+ min^{-1} mg^{-1} protein) measured via a Coomassie Plus™ (Bradford) Assay Kit (Thermo Scientific).

Membrane CA activity

For heart and red muscle tissue, cytoplasmic and membrane fractions were obtained using differential centrifugation methods as previously described (e.g. Esbaugh and Tufts, 2006; McMillan et al., 2019). Tissue was added to 8 volumes of ice-cold buffer medium per gram of tissue and homogenized until no pieces of tissue remained. Crude homogenate was centrifuged to remove cellular debris and mitochondrial components (7500 ***g*** for 20 min at 4°C). The supernatant was removed and centrifuged (100,000 ***g*** for 90 min at 4°C, Beckman L7-55 ultracentrifuge) again to separate membrane and cytoplasmic fractions, where we expect to find membrane-bound CA-IV and cytoplasmic CA, respectively. To ensure true measurement of membrane-bound CA activity with no influence of cytoplasmic CA, membrane fractions were 'washed' according to Esbaugh and Tufts (2006). The pellet was resuspended in buffer medium, agitating the sample with mild sonication, and pelleted again by ultracentrifugation (100,000 ***g*** for 90 min at 4°C). CA activity of the cytoplasm and membrane fractions for both heart and red muscle tissue was measured using the electrometric pH method described above. To confirm whether the CA activity measured was cytoplasmic or membrane bound, all samples went through an additional inhibition trial with SDS (0.005%), a potent detergent that inhibits cytoplasmic CA but does not affect membrane-bound CA (Whitney and Briggle, 1982). To determine the effect of SDS on CA activity, the SDS-treated reaction rate was divided by the control (untreated) catalyzed reaction rate (µmol H^+ min^{-1} mg^{-1} protein) and multiplied by 100. Data are presented as CA activity relative to control (%). Therefore, if CA activity is not affected by SDS (i.e. membrane-bound CA), CA activity relative to control would be 100%.

Statistical analyses

Analyses were performed using R Studio (version 4.0.2; https://www.rstudio.com/). All data were assessed for normality and homogeneity of variance prior to analyses. One outlier was removed from the red muscle CA inhibition dataset prior to analyses, as it was biologically improbable (where CA activity increased 470% with SDS). There were no statistical differences between replicate tanks and all following tests were performed on individuals. A Student's *t*-test (α=0.05) was used to determine the effect of treatment on RBC CA activity at 8 days. To determine the effects of treatment and subcellular location (i.e. membrane or cytoplasm) on CA activity and CA inhibition by SDS, Type III two-way ANOVA (α=0.05) were used. Tukey *post hoc* analyses were carried out when an interaction effect was detected.

Series III: whole-animal respiratory performance

Critical swim performance test

Red drum were held in ∼250 l recirculating tanks (34 ppt; 23.4±0.1°C) and were fed *ad libitum* until the 48 h prior to swim trials. Fish were exposed in either chronic normoxia (n=9, mass: 58.0±3.2 g, total length, TL: 18.9±0.4 cm, DO: 99.9±0.3%, pH: 8.06±0.01) or hypoxia (n=7, mass: 55.4±4.8 g, TL: 18.4±0.5 cm, DO: 31.8±0.3%, pH: 7.85±0.01) as described for series I.

Oxygen consumption ($\dot{M}_{O_2}$; mg O_2 kg^{-1} h^{-1}) and critical swim speed [U_{crit}; body lengths (BL) s^{-1}] were measured under normoxia for each individual at day 8 of treatment using a 5 l clear acrylic swim respirometer (working section 22.0×7.5×6.0 cm; Loligo® Systems). Flow velocity within the respirometer was calibrated using a digital flow meter (Hontzsch, Germany), and solid blocking effects from the fish's body were taken into account according to Bell and Terhune (1970). For each individual, the respirometer was filled with clean, fully aerated seawater and the temperature (24.0±0.3°C) was controlled with a temperature controller (Willhi). The respirometer was covered with bubble wrap to prevent surface mixing, with the exception of a window directly above the working area containing the fish to video record swim behavior. On day 7 of normoxia or hypoxia exposure, fish were transferred to the respirometer of their respective treatment condition and allowed to acclimate overnight (at least 12 h) at a swimming speed of 0.5 BL s^{-1}. For hypoxia-acclimated fish, hypoxic DO (32.8±0.1%) was maintained in the respirometer using the Oxy-Reg systems (Loligo® Systems) described in series I. $\dot{M}_{O_2}$ was measured within the respirometer using a fiber optic oxygen meter (Witrox, Loligo® Systems), and collected in real time with Autoresp v.2.2.2 (Loligo® Systems). Respirometry cycles during the acclimation period for both treatments consisted of a 2 min flush, 30 s wait and 2.5 min measure period (5 min cycle total). This ensured O_2 levels for the hypoxia treatment did not decrease below 25% air saturation overnight, which would approach P_{crit} for the species (Pan et al., 2016), and to maintain r^2 values above 0.95. The following morning, DO for hypoxia-acclimated

Journal of Experimental Biology (2022) 225, jeb244474. doi:10.1242/jeb.244474

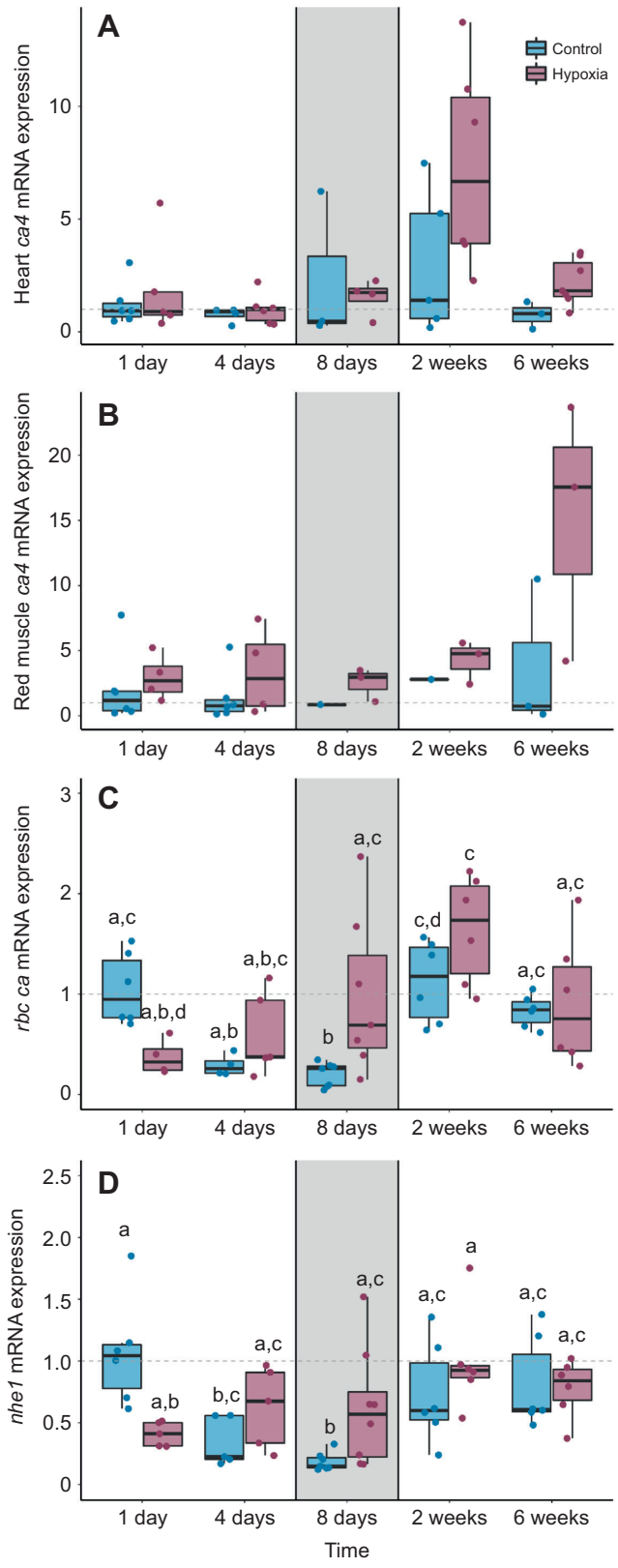

Fig. 1. Comparison of relative mRNA expression for genes involved in tissue oxygen extraction in red drum acclimated to control seawater or hypoxia over 6 weeks. Relative mRNA expression for (A) heart *ca4*, (B) red muscle *ca4*, (C) *rbc ca* and (D) *nhe1*. Heart (A) and red muscle (B) *ca4* expression was not significantly affected by treatment or time, nor was there an interaction between the two factors (two-way ANOVA, $P>0.05$). Red drum exposed to prolonged hypoxia demonstrate phenotypic changes by 8 days in a companion study (Negrete et al., 2022), thus changes to *ca4, rbc ca* and *nhe1* were expected to occur by 8 days (highlighted in grey). *rbc ca* expression (C) was significantly affected by hypoxia treatment (two-way ANOVA, $P<0.01$) and time ($P<0.01$), and there was a significant interaction between treatment and time ($P<0.01$). Hypoxia-acclimated fish demonstrated downregulation of *rbc ca* at 1 day compared with control fish, and significantly higher *rbc ca* expression at 8 days compared with control fish (Tukey HSD, $P<0.05$). *nhe1* expression (D) was significantly affected by hypoxia treatment (two-way ANOVA, $P<0.01$) and time ($P<0.01$), and there was a significant interaction between treatment and time ($P<0.01$). Hypoxia-acclimated fish had significantly higher *nhe1* expression in RBCs compared with control fish at 8 days (Tukey HSD, $P<0.05$). Expression was calculated relative to *ef1α* and normalized using control 1 day expression for each tissue type and gene. Box plots show minimum, first quartile, median, third quartile and maximum for each treatment (control in blue, hypoxia in pink). Individual data points are shown (n=6–8 per treatment and time point, except where no Ct value or outlier was present). Letters denote significant differences as detected by Tukey *post hoc* analysis.

fish was increased to 100% over 1 h (10% increase every 10 min) prior to initiating the U_{crit} trial.

$\dot{M}_{O_2}$ was measured at increasing speeds (generally 0.5–5.0 BL s^{-1}), with 0.5 BL s^{-1} speed increments for a total of 20 min at each speed. This allowed a total of four $\dot{M}_{O_2}$ measurements per swim speed (measurement intervals as described above). The U_{crit} trial was terminated when the fish could no longer swim against the flow and either fell to the back on the retaining grid for >5 s or maintained slow caudal fin movement while propped against the retaining grid, resulting in a reduced $\dot{M}_{O_2}$. Swim speed (BL s^{-1}) and total time at speed were recorded, after which the flow was slowly returned to 0.5 BL s^{-1} for 30 min. Afterwards, the fish was removed from the respirometer and returned to a normoxia holding tank.

Background O_2 consumption was measured before and after the fish was introduced into the respirometer to account for bacterial respiration. Background respiration was measured with cycles of 3 min flush, 1 min wait and 26 min measurement periods at 0.5 BL s^{-1}. For each trial, $\dot{M}_{O_2}$ was corrected using the average start and end background $\dot{M}_{O_2}$.

Calculations and statistical analyses

U_{crit} was calculated as per Brett (1964):

$$U_{crit} = U + \left(U_i \times \frac{t}{t_i}\right), \quad (2)$$

where U is the penultimate swim speed before the fish stopped swimming, U_i is the swim speed increment (0.5 BL s^{-1}), t is the length of time in the final increment where failure occurred, and t_i is the time interval for each swim speed (20 min). U_{burst}, the speed at which the fish transitions to burst-and-coast swimming, was calculated with the same equation where U is the penultimate swim speed before the fish started burst-and-coast swimming, and t is the length of time in the final increment where burst-and-coast swimming occurred. To determine standard metabolic rate (SMR), an exponential regression was fitted by least squares to average $\dot{M}_{O_2}$ at each swimming speed:

$$\dot{M}_{O_2} = a + bU^c, \quad (3)$$

where a, b and c are constants (Claireaux et al., 2006). SMR was determined by extrapolating $\dot{M}_{O_2}$ to zero swimming speed, i.e. the y-intercept (Claireaux et al., 2006; Johansen and Esbaugh, 2017).

Journal of Experimental Biology (2022) 225, jeb244474. doi:10.1242/jeb.244474

Using this equation and the resulting constants, maximum metabolic rate (MMR) was calculated as the $\dot{M}_{O_2}$ at U_{crit}. MMR and SMR were mass-corrected using the scaling exponents previously determined for red drum (Ackerly and Esbaugh, 2020; Pan et al., 2016). Absolute aerobic scope (AAS) was calculated as MMR−SMR, and factorial aerobic scope (FAS) as MMR/SMR. Also, routine metabolic rate (RMR) was measured for normoxia-acclimated fish as the average of all $\dot{M}_{O_2}$ points observed during the overnight acclimation period, from the start of respirometry to the start of the swim trial. In the case of hypoxia-acclimated fish, RMR was calculated from the start of respirometry to the start of reoxygenation 1 h prior to the swim trial.

To calculate the optimum swim speed (U_{opt}; the speed at which energy expenditure is minimized per unit of travel distance) the constants a, b and c from the Eqn 3 were transformed as per Videler (1993):

$$U_{opt} = \left[\frac{a}{(c-1)\times b}\right]^{\frac{1}{c}}. \quad (4)$$

To determine swimming efficiency, cost of transport (COT; J km^{-1} kg^{-1}) was calculated for U_{crit}, U_{opt} and U_{burst}. As per Claireaux et al. (2006), $\dot{M}_{O_2}$ at U_{crit}, U_{opt} or U_{burst} was converted from mg O_2 kg^{-1} h^{-1} to J kg^{-1} h^{-1}, and divided by swim speed (U_{crit}, U_{opt} or U_{burst}; converted from BL s^{-1} to km h^{-1} using individual fish TL).

Calculations and statistical analyses were performed using R Studio (version 4.0.2; https://www.rstudio.com/). Prior to analysis, all data were assessed for normality and homogeneity of variance. One outlier was identified and removed from the U_{crit} (and subsequently COT at U_{crit}, COT_{Ucrit}) dataset, where the fish preemptively failed without displaying burst swim behavior. Similarly, one outlier was removed from the U_{opt} (and subsequently COT at U_{opt}, COT_{Uopt}) dataset, where calculated U_{opt} was greater than U_{crit} (biologically improbable). There were no statistical differences between replicate tanks and all following tests were performed on individuals. One-tailed t-tests (α=0.05) were used to assess the effect of hypoxia treatment on MMR, U_{crit} and U_{opt} as increased O_2 extraction efficiency was expected to increase these performance metrics. Student's t-tests (α=0.05) were used for the following measurements: RMR, SMR, AAS, FAS, U_{burst}, COT_{Ucrit}, COT_{Uopt} and COT_{Uburst}.

RESULTS

Gene expression

There was no significant effect of hypoxia on heart *ca4* mRNA expression at 1 day, 4 days, 8 days, 2 weeks or 6 weeks (Fig. 1A; two-way ANOVA, $F_{1,39}$=0.11, P=0.75) nor was there a significant effect of time ($F_{4,39}$=0.71, P=0.59). There was no interaction between treatment and time for heart *ca4* mRNA expression ($F_{4,39}$=1.13, P=0.36). Similarly, while hypoxia-acclimated fish trended toward greater *ca4* expression in red muscle than control fish, treatment was not statistically significant (Fig. 1B; two-way ANOVA, $F_{1,24}$=1.32, P=0.26) nor was time ($F_{4,24}$=0.27, P=0.89), and treatment and time did not have an interaction effect ($F_{4,24}$=0.54, P=0.71). *rbc ca* gene expression was significantly affected by hypoxia treatment (Fig. 1C; two-way ANOVA, $F_{1,47}$=7.40, P<0.01) and time ($F_{4,47}$=12.37, P<0.01), and there was a significant interaction between treatment and time ($F_{4,47}$=6.92, P<0.01). *Post hoc* analysis revealed that hypoxia-acclimated fish demonstrated downregulation of *rbc ca* at 1 day compared with control fish, and expression increased at 4 days, 8 days and 2 weeks. Control fish significantly downregulated *rbc ca* expression at 8 days, and at this time-point, hypoxia-acclimated fish had significantly higher *rbc ca* expression compared with control fish (Tukey HSD, P<0.05). *nhe1* gene expression was significantly affected by hypoxia treatment (Fig. 1D; two-way ANOVA,

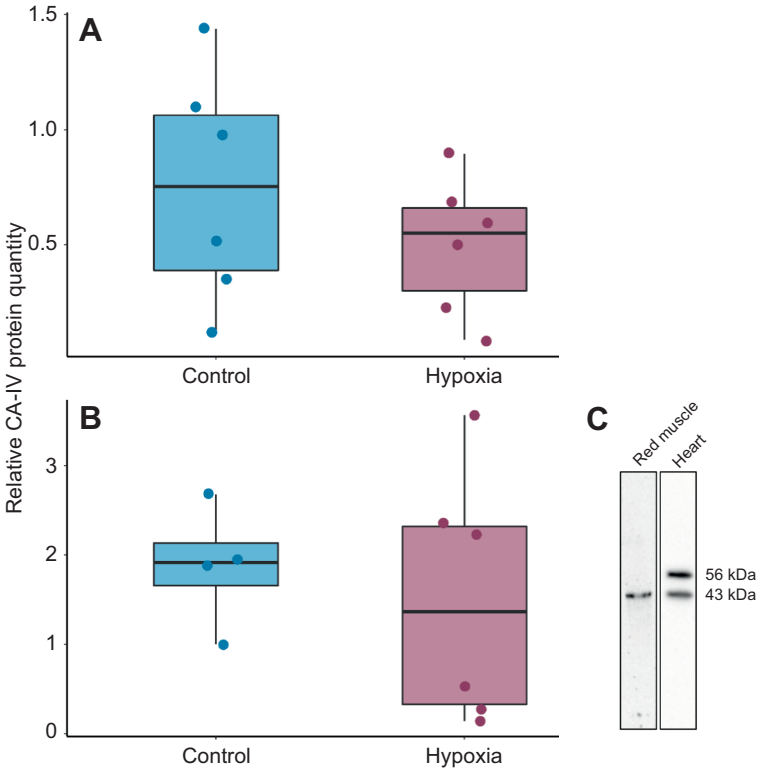

Fig. 2. Comparison of plasma-accessible carbonic anhydrase (CA-IV) protein quantity in the heart and red muscle tissue of red drum acclimated to control seawater or hypoxia for 8 days. (A,B) There were no significant differences in mature CA-IV protein levels between treatments for heart (A; Student's t-test, P=0.32) or red muscle (B; Student's t-test, P=0.64). CA-IV protein content and total protein content of each sample were calculated relative to control at 8 days (C1A8D) using either heart or red muscle as appropriate. Relative CA-IV protein content was normalized to relative total protein content for each sample to account for any overall reduction in protein due to hypoxia exposure. Therefore, the relative protein quantity of C1A8D is 1 for both red muscle and heart. Box plots show minimum, first quartile, median, third quartile and maximum for each treatment (control in blue, hypoxia in pink). Individual data points are shown (n=4–6 per treatment). (C) Representative western blot images showing that red muscle CA-IV appeared as a single 43 kDa band, and heart CA-IV appeared as both 56 kDa and 43 kDa bands. Relative protein quantity was assessed for the 43 kDa band for both tissues, as this was considered the mature form of CA-IV protein.

Journal of Experimental Biology (2022) 225, jeb244474. doi:10.1242/jeb.244474

$F_{1,50}$=8.32, P<0.01) and time ($F_{4,50}$=11.85, P<0.01), and there was a significant interaction between treatment and time ($F_{4,50}$=5.66, P<0.01). Similar to *rbc ca* expression, control fish demonstrated downregulation at 4 days and 8 days. Hypoxia-acclimated fish generally maintained *nhe1* expression over time, and at 8 days had significantly higher expression than control fish (Tukey HSD, P<0.05).

Phenotype assessment

The hypoxia-induced phenotype was tested using a combination of western blots, immunohistochemistry and enzyme analysis at 8 days of acclimation. This time point was chosen based on the significant up-regulation in *rbc CA* and *nhe1*, which coincided with prior work on the effects of hypoxia-induced Hb plasticity on aerobic performance in red drum (see Discussion). In agreement with mRNA results, western blots did not demonstrate any change to CA-IV protein abundance in the heart (Fig. 2A; Student's *t*-test, t=1.05, P=0.32, d.f.=10) and red muscle (Fig. 2B; t=0.48, P=0.64, d.f.=8). Immature CA-IV protein abundance was significantly lower in the heart under hypoxia (Fig. S5; Student's *t*-test, t=2.61, P=0.03, d.f.=10). Note that no antibody is currently available for NHE1 in red drum, and protein abundance for RBC CA was only tested using enzyme activity.

Qualitative analysis of confocal images demonstrated no visible difference in CA-IV localization between control and hypoxia-acclimated fish at 8 days (Fig. 3). Immunofluorescence images were

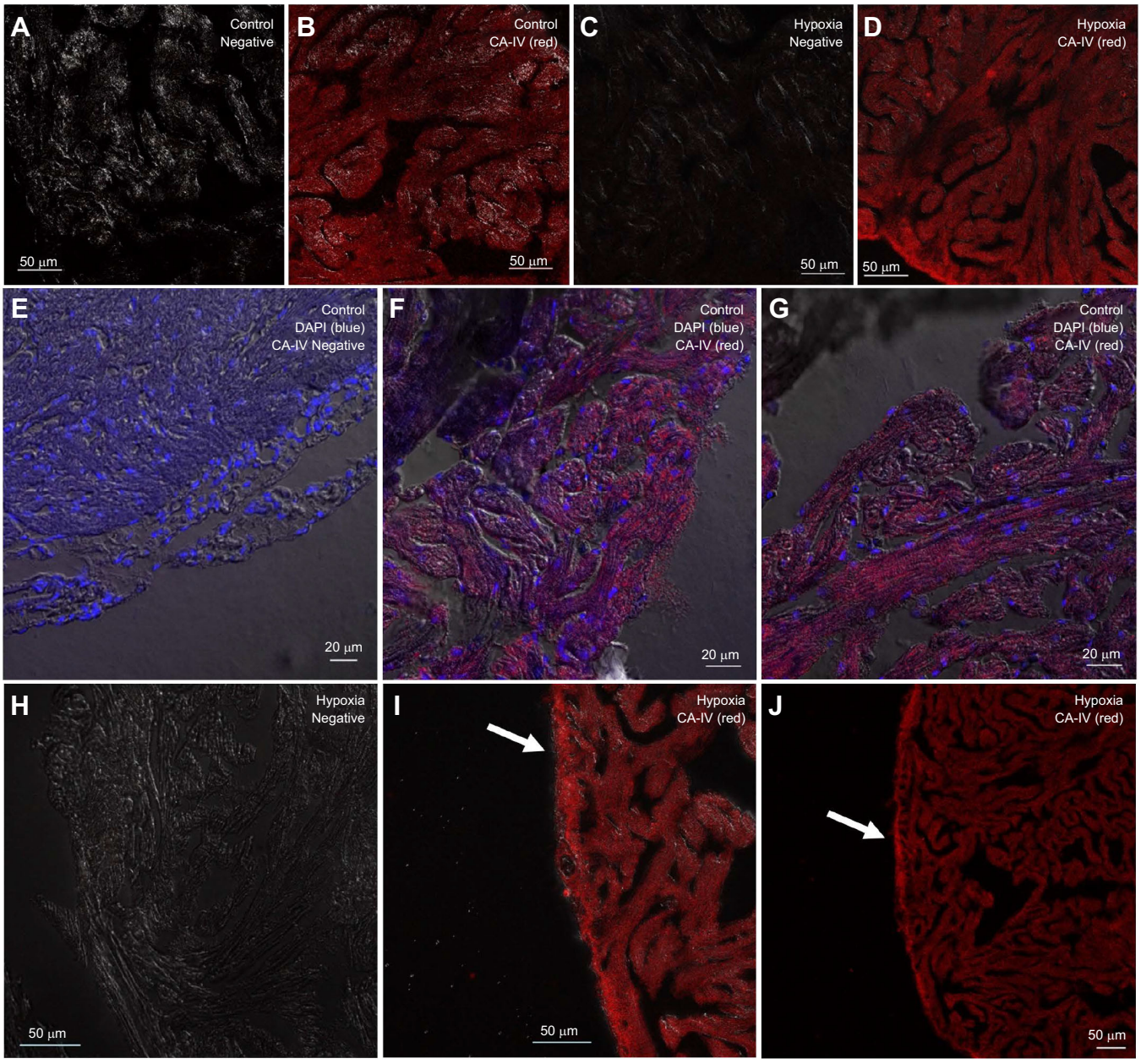

Fig. 3. Representative immunofluorescence images of ventricles of red drum acclimated to control seawater or hypoxia for 8 days. CA-IV (red) appears to be diffuse throughout the ventricle for both control (B,F,G) and hypoxia (D,I,J) treatment in all images, with a stronger signal on the epicardium rather than the spongy myocardium (indicated with an arrow in I and J). The no-primary antibody (negative) controls (A,C,E,H) did not show any CA-IV immunofluorescence. All fluorescence images were overlayed with differential interference contrast images.

Journal of Experimental Biology (2022) 225, jeb244474. doi:10.1242/jeb.244474

overlayed with differential interference contrast (DIC) images. No-primary antibody controls did not show any CA-IV immunofluorescence. Interestingly, CA-IV appears to be diffuse throughout the ventricle, with a stronger signal on the outer compact myocardial layer rather than the spongy myocardium (Fig. 3I,J). To our knowledge, this study represents the first use of a CA-IV antibody in a teleost heart.

Despite the increase in *rbc ca* gene transcript abundance at 8 days in hypoxia-acclimated fish, RBC CA activity was not significantly affected by hypoxia treatment (Fig. 4; Student's *t*-test, $t=-0.80$, $P=0.43$, d.f.=22). Similarly, hypoxia treatment did not have an effect on CA activity in heart or red muscle membrane or cytoplasmic fractions. SDS – an inhibitor of CA activity that is not effective on membrane isoforms – was also used to validate the presence of membrane-bound CA in the heart and red muscle of red drum. As we expected, cytoplasmic CA activity was significantly inhibited and CA activity in membrane fractions was not (Fig. 5A; two-way ANOVA, $P<0.001$). Hypoxia acclimation had no effect on the response of CA activity to SDS treatment ($F_{1,27}=0.44$, $P=0.51$) nor was there an interaction between subcellular location and hypoxia treatment ($F_{1,27}=0.003$, $P=0.96$). Similarly, red muscle cytoplasmic CA activity was significantly inhibited while membrane CA activity was not (Fig. 5B; two-way ANOVA, $P<0.001$). Hypoxia acclimation did not have a significant effect ($F_{1,27}=0.23$, $P=0.64$) nor was there an interaction between subcellular location and hypoxia treatment ($F_{1,27}=0.47$, $P=0.50$).

In both acclimation treatments, CA activity was significantly different between membrane and cytoplasmic fractions (Fig. 5C; two-way ANOVA, $P<0.001$), where membrane CA activity (control: 13.7±4.5 µmol H^+ min^{-1} mg^{-1} protein; hypoxia: 8.1±1.7 µmol H^+ min^{-1} mg^{-1} protein) was significantly less than cytoplasmic CA activity (control: 147.9±63.4 µmol H^+ min^{-1} mg^{-1} protein; hypoxia: 134.3±39.9 µmol H^+ min^{-1} mg^{-1} protein). There was no significant effect of hypoxia treatment ($F_{1,28}=0.14$, $P=0.71$) nor an interaction between subcellular location and hypoxia treatment ($F_{1,28}=0.65$, $P=0.43$). Similar findings were observed in the red muscle, with a significant difference in activity between the membrane and cytoplasmic fractions (Fig. 5D; two-way ANOVA, $P<0.001$), where membrane CA activity (control: 9.7±1.8 µmol H^+ min^{-1} mg^{-1} protein; hypoxia: 6.7±2.4 µmol H^+ min^{-1} mg^{-1} protein) was significantly less than cytoplasmic CA activity (control: 81.7±10.4 µmol H^+ min^{-1} mg^{-1} protein; hypoxia: 83.2±12.1 µmol H^+ min^{-1} mg^{-1} protein). Again, there was no significant effect of hypoxia treatment ($F_{1,28}=1.09$, $P=0.31$) nor an interaction between subcellular location and hypoxia treatment ($F_{1,28}=0.87$, $P=0.36$).

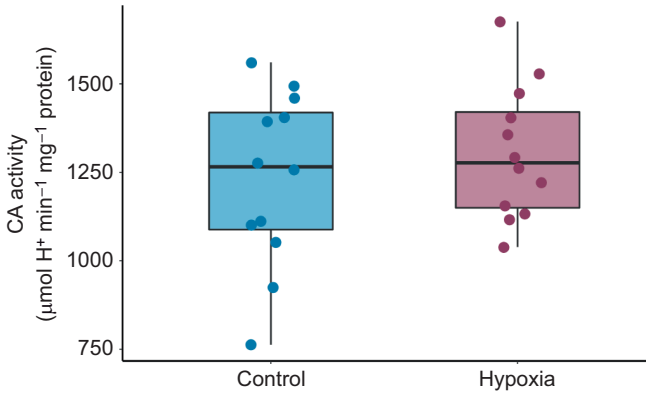

Fig. 4. Comparison of red blood cell carbonic anhydrase activity of red drum acclimated to control seawater or hypoxia for 8 days. Although there was an increase in *rbc ca* gene expression at 8 days (see Fig. 1C), red blood cell (RBC) carbonic anhydrase (CA) activity was not significantly affected by hypoxia treatment (Student's *t*-test, $P=0.43$). Box plots show minimum, first quartile, median, third quartile and maximum for each treatment (control in blue, hypoxia in pink). Individual data points are shown ($n=12$ per treatment).

Whole-animal respiratory performance

Metabolic and swim performance in normoxic water was assessed following 8 days of hypoxia acclimation (Table 2). RMR was not significantly different between control and hypoxia-acclimated fish (Student's *t*-test, $t=0.42$, $P=0.68$, d.f.=14). MMR was not significantly different between control and hypoxia-acclimated fish (Fig. 6A; one-tailed *t*-test, $t=-0.20$, $P=0.58$, d.f.=6). SMR was not significantly different between control and hypoxia-acclimated fish (Fig. 6B; Student's *t*-test, $t=1.12$, $P=0.28$, d.f.=14). AAS was not significantly different between treatments (Fig. 6C; Student's *t*-test, $t=-0.13$, $P=0.90$, d.f.=14). FAS was not significantly different between treatments (Fig. 6D; Student's *t*-test, $t=-0.69$, $P=0.50$, d.f.=14).

U_{crit} was significantly different between treatments (Table 2, Fig. 7A; one-tailed *t*-test, $t=2.34$, $P=0.03$, d.f.=6), where hypoxia-acclimated fish obtained significantly higher U_{crit} in normoxia compared with normoxia-acclimated fish (5.11±0.13 BL s^{-1} and 4.81±0.08 BL s^{-1}, respectively). COT_{Ucrit} was not significantly different between treatments (Fig. 7B; Student's *t*-test, $t=0.78$, $P=0.45$, d.f.=13). U_{opt} was not significantly different between treatments (Fig. 7C; one-tailed *t*-test, $t=1.59$, $P=0.09$, d.f.=5), nor was COT_{Uopt} (Fig. 7D; Student's *t*-test, $t=-1.65$, $P=0.12$, d.f.=14). U_{burst} was not significantly different between treatments (Fig. 7E; Student's *t*-test, $t=0.15$, $P=0.88$, d.f.=13), nor was COT_{Uburst} (Fig. 7F; Student's *t*-test, $t=0.41$, $P=0.69$, d.f.=13).

DISCUSSION

The overall aim of this study was to determine whether red drum elevated their capacity for tissue O_2 extraction in the heart and red muscle following acclimation to prolonged environmental hypoxia, and, if so, whether this benefited whole-animal aerobic metabolism and swim performance. Contrary to previous findings in rainbow trout (Harter et al., 2019), our results suggest that red drum do not improve tissue O_2 extraction metrics – such as CA-IV and RBC CA – following hypoxia acclimation, nor did fish exhibit any change in SMR, MMR or AS. Surprisingly, hypoxia-acclimated fish did improve critical swim performance despite the unaffected MMR. In lieu of improvements to O_2 transport capacity, this improved swim performance was instead driven by improved anaerobic performance.

Previous studies have demonstrated a critical role for red muscle and heart CA-IV in enhanced tissue O_2 extraction by increasing local O_2 partial pressure gradients via βNHE short-circuiting (Alderman et al., 2016; Harter et al., 2019; Rummer and Brauner, 2011, 2015; Rummer et al., 2013). While it has been suggested that increased CA-IV abundance may improve tissue O_2 extraction under hypoxia, we present one of the first studies to investigate this concept, characterizing membrane-bound CA in the red muscle and heart of red drum. Western blots demonstrated specificity for CA-IV, and resistance to SDS treatment confirmed the isoform was membrane associated. The diffuse nature of CA-IV staining in the cardiac trabeculae is somewhat surprising, though few studies have visualized CA-IV distribution. In rainbow trout (*Oncorhynchus mykiss*) proximal kidney tubules, CA-IV appears similarly diffuse, and in coho salmon (*Oncorhynchus kisutch*) heart, CA-IV is diffuse

Journal of Experimental Biology (2022) 225, jeb244474. doi:10.1242/jeb.244474

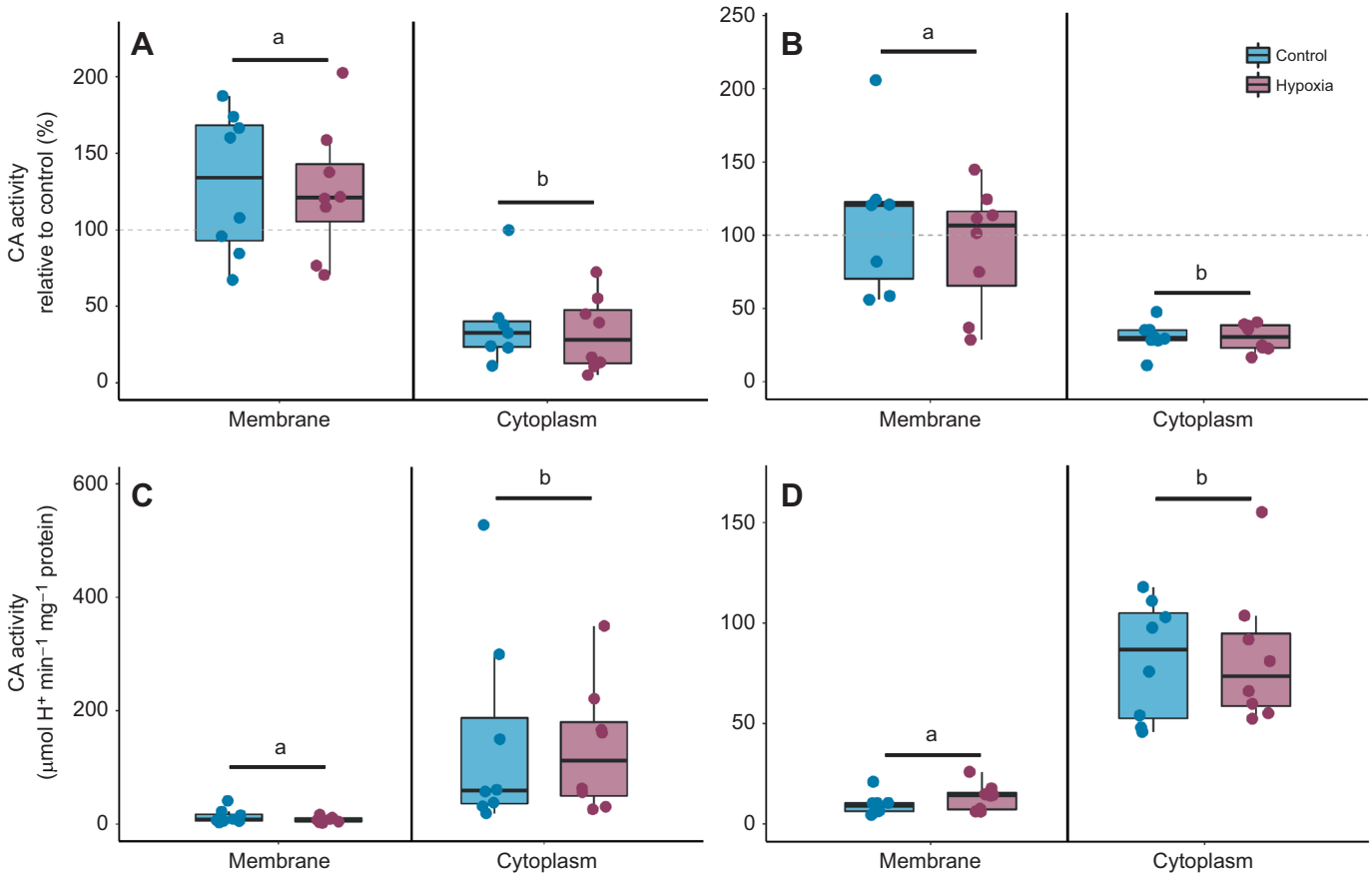

Fig. 5. Determination of CA membrane association and activity in the heart and red muscle of red drum acclimated to control seawater or hypoxia for 8 days. Membrane and cytoplasmic fractions were treated with SDS, a potent cytoplasmic CA inhibitor, and CA activity was determined. (A,B) To determine the effect of SDS on CA activity, the SDS-treated reaction rate was divided by the untreated control reaction rate (μmol H^+ min^{-1} mg^{-1} protein) and multiplied by 100; data are presented as CA activity relative to control (%). SDS treatment had a significant effect on subcellular location in the heart (A; two-way ANOVA, P<0.001). Cytoplasmic CA activity was significantly inhibited (control: 38.7±10.9%; hypoxia: 32.2±8.6%), and membrane fraction CA activity was not (control: 130.5±16.5%; hypoxia: 125.4±15.1%). Similarly, red muscle subcellular location was significantly affected by SDS treatment (B; two-way ANOVA, P<0.001), where only cytoplasmic CA activity was significantly inhibited (control: 30.7±3.6%; hypoxia: 30.2±3.3%) and membrane CA activity was not (control: 109.8±19.5%; hypoxia: 92.1±14.7%). This verifies the membrane fraction represents membrane-bound CA-IV protein. Hypoxia acclimation had no effect on CA activity when treated with SDS nor was there an interaction between hypoxia acclimation and subcellular location for either heart or red muscle (P>0.05). (C,D) CA activity (μmol H^+ min^{-1} mg^{-1} protein) of the cytoplasmic fraction was significantly higher than that of the membrane fraction for both heart (C) and red muscle tissue (D; two-way ANOVA, P<0.001) but there were no significant effects of hypoxia treatment nor was there an interaction between subcellular location and hypoxia treatment for either heart or red muscle (P>0.05). Box plots show minimum, first quartile, median, third quartile and maximum for each treatment (control in blue, hypoxia in pink). Individual data points are shown (n=7–8 per treatment). Letters denote significant differences between subcellular locations.

in the outer compact layer of the myocardium but is highly localized in the spongy layer (Alderman et al., 2016; Georgalis et al., 2006). These variations in staining may be attributed to differences in species, tissues, staining techniques and/or antibody specificity (i.e. staining of mature and immature membrane-bound CA), but more research is necessary to understand these differences. Despite this evidence for the presence of CA-IV across levels of biological organization, there was no significant effect of hypoxia acclimation on mRNA transcript abundance for CA-IV, nor was there an increase in mature CA-IV protein abundance or membrane-bound CA activity. It is interesting to note immature CA-IV protein decreased in the heart at 8 days under hypoxia, contrary to the prediction that red drum would upregulate CA-IV during hypoxia acclimation if they utilized enhanced tissue O_2 extraction to support acclimation. The mRNA expression of *nhe1* and *rbc ca* – two proteins also involved in the proposed tissue O_2 extraction mechanism – increased at 4 days, 8 days and 2 weeks in hypoxia-acclimated fish. Yet, RBC CA activity did not increase with hypoxia acclimation, and a suitable antibody to quantify NHE1 protein is not available for red drum. As such, it seems clear that despite some transcriptional support for our hypothesis, red drum do not alter the biochemical components for tissue O_2 extraction during hypoxia acclimation.

Our study built on previous work by Harter et al. (2019) that suggested that CA-IV expression may be a plastic trait that fish can benefit from when O_2 demand is high. Normoxia- and hypoxia-acclimated rainbow trout (*O. mykiss*) increased cardiac output in response to CA-IV inhibition during a swim trial (at 50% U_{crit}) while $\dot{M}_{O_2}$ was maintained. Using the Fick equation for theoretical support, Harter et al. (2019) suggested that cardiac output increased to compensate for a reduction in tissue O_2 extraction caused by membrane-bound CA inhibition, thus demonstrating the functional role of membrane-bound CA in both normoxia- and hypoxia-acclimated fish. The authors demonstrated hypoxia-acclimated trout relied on CA-IV during recovery from exhaustive exercise and from CA-IV inhibition more so than their normoxia-acclimated counterparts. During recovery, $\dot{M}_{O_2}$ was again maintained across

Journal of Experimental Biology (2022) 225, jeb244474. doi:10.1242/jeb.244474

Table 2. Comparison of metabolic and swim performance of red drum under normoxic conditions after acclimation to control seawater or hypoxia (32% dissolved oxygen) for 8 days

Performance metric	Control	Hypoxia
RMR (mg O_2 kg^{-1} h^{-1})	159.7±7.7 (9)	154.3±10.6 (7)
SMR (mg O_2 kg^{-1} h^{-1})	134.8±9.9 (9)	118.5±10.6 (7)
MMR (mg O_2 kg^{-1} h^{-1})	513.1±31.5 (9)	504.5±43.6 (7)
AAS (mg O_2 kg^{-1} h^{-1})	378.3±37.8 (9)	386.0±46.6 (7)
FAS (MMR/SMR)	4.02±0.41 (9)	4.50±0.60 (7)
U_{crit} (BL s^{-1})	4.81±0.08 (8)	5.11±0.13 (7)*
COT_{Ucrit} (J kg^{-1} km^{-1})	2138.7±108.0 (8)	1996.6±151.1 (7)
U_{opt} (BL s^{-1})	2.67±0.12 (8)	3.15±0.30 (6)
$COT_{U_{opt}}$ (J kg^{-1} km^{-1})	1501.5±132.7 (8)	1807.1±118.8 (6)
U_{burst} (BL s^{-1})	4.21±0.14 (8)	4.17±0.23 (7)
$COT_{U_{burst}}$ (J kg^{-1} km^{-1})	1904.6±81.4 (8)	1853.3±97.9 (7)

Metabolic performance metrics are: routine metabolic rate (RMR), standard metabolic rate (SMR), maximum metabolic rate (MMR), absolute aerobic scope (AAS) and factorial aerobic scope (FAS). MMR and SMR were mass-corrected using the scaling exponents previously determined for red drum (Ackerly and Esbaugh, 2020; Pan et al., 2016). Swim performance metrics are: critical swim speed (U_{crit}), cost of transport at critical swim speed (COT_{Ucrit}), optimal swim speed (U_{opt}), cost of transport at optimal swim speed (COT_{Uopt}), burst swim speed (U_{burst}) and cost of transport at burst swim speed (COT_{Uburst}). Data are means±s.e.m., with sample sizes for each measure in parentheses. *Statistically significant difference between control and hypoxia-acclimated fish (one-tailed *t*-test, $P<0.05$).

both treatment groups, but while cardiac output returned to resting levels in normoxia-acclimated fish, cardiac output only decreased ~10% in hypoxia-acclimated fish. Harter et al. (2019) thus suggested that fish may recruit and rely more heavily on CA-IV for tissue O_2 extraction to maintain $\dot{M}_{O_2}$ under hypoxia, especially during recovery from exhaustive exercise. The data presented here for red drum conflict with the hypothesis of Harter et al. (2019) as membrane-bound CA abundance and activity in the heart and red muscle was unaffected by hypoxia. It should be noted that maintenance of CA-IV may still represent a mechanism employed by fish to maintain $\dot{M}_{O_2}$. Importantly, this work represents the first exploration of CA-IV-mediated O_2 extraction in the heart and red muscle of a non-salmonid, which may explain the difference in their response to hypoxia and use of enhanced tissue O_2 extraction in general. Firstly, the cardiac morphology of red drum would best be described as a 'type 1' heart, whereby the ventricle is primarily made up of spongy myocardium with little compact myocardium or coronary circulation. Species with type 1 hearts are generally considered to be less athletic when compared with salmonids and other species with a higher proportion of compact myocardium (reviewed by Farrell, 2007). Efficient tissue O_2 extraction is indeed beneficial to alleviate aerobic constraints during exercise, but in non-athletic species that are routinely exposed to environmental O_2 limitations, efficient O_2 uptake may take precedence.

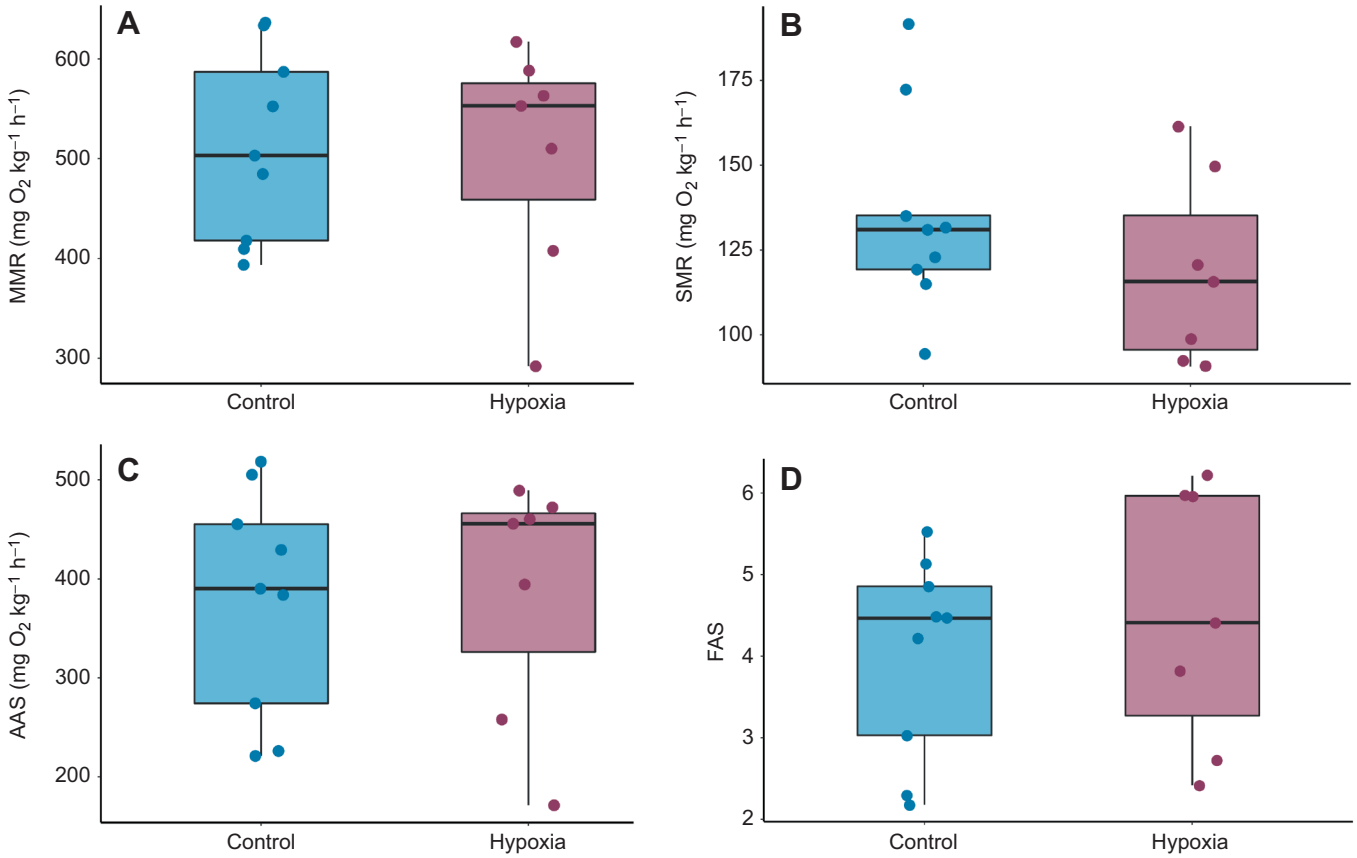

Fig. 6. Metabolic performance of red drum under normoxic conditions after acclimation to control seawater or hypoxia for 8 days. Oxygen consumption ($\dot{M}_{O_2}$; mg O_2 kg^{-1} h^{-1}) was measured during critical swim speed (U_{crit}) trials. (A) Maximum metabolic rate (MMR) was calculated as the $\dot{M}_{O_2}$ at the fish's U_{crit}. (B) Standard metabolic rate (SMR) was calculated as the $\dot{M}_{O_2}$ at zero swimming speed. MMR and SMR were mass-corrected using the scaling exponents previously determined for red drum (Ackerly and Esbaugh, 2020; Pan et al., 2016). (C) Absolute aerobic scope (AAS) was measured as the difference between MMR and SMR. (D) Factorial aerobic scope (FAS) was measured as the ratio between MMR and SMR. Box plots show minimum, first quartile, median, third quartile and maximum for each treatment (control in blue, hypoxia in pink). Individual data points are shown (n=7–9 per treatment). There were no statistically significant differences between the metabolic performance of control and hypoxia-acclimated fish under normoxia (one-tailed *t*-test for MMR and two-tailed *t*-tests for SMR, AAS, FAS; $P>0.05$).

Journal of Experimental Biology (2022) 225, jeb244474. doi:10.1242/jeb.244474

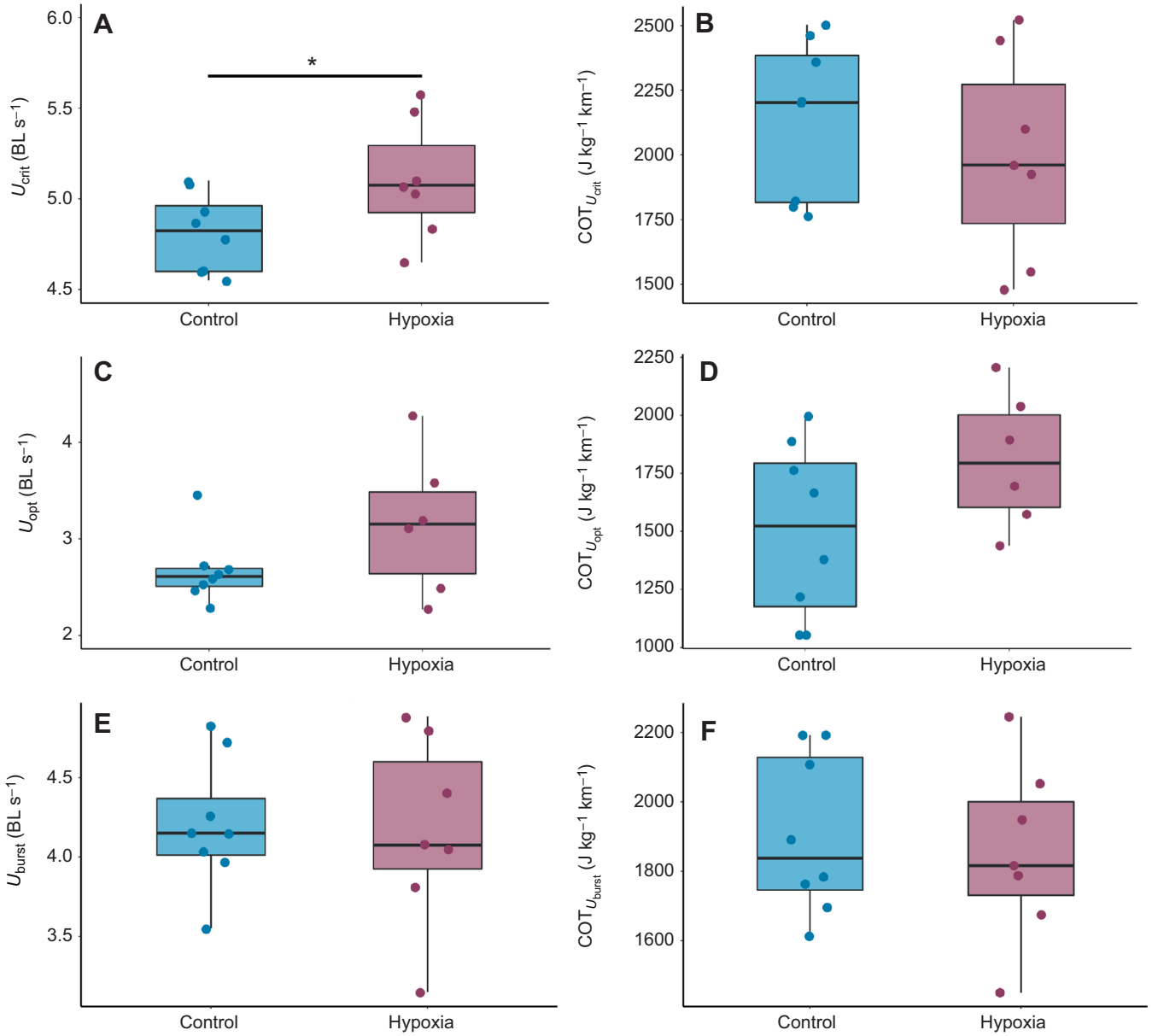

Fig. 7. Swim performance of red drum under normoxic conditions after acclimation to control seawater or hypoxia for 8 days. Swimming respirometry was used to measure critical swim speed (U_{crit}), optimal swim speed (U_{opt}) and burst swim speed (U_{burst}) [in body lengths (BL) per second] for control and 8 day hypoxia-acclimated fish under normoxia. The cost of transport (COT), a measure of swimming efficiency, was also calculated for each swim speed measurement. (A) U_{crit} was significantly different between treatments (one-tailed *t*-test, P=0.03), where hypoxia-acclimated fish obtained significantly higher U_{crit} in normoxia. (B) COT at U_{crit} was not significantly different between treatments (Student's *t*-test, P=0.45). (C) U_{opt} was not significantly different between treatments (one-tailed *t*-test, P=0.09). (D) COT at U_{opt} was not significantly different between treatments (Student's *t*-test, P=0.12). (E) U_{burst} was not significantly different between treatments (Student's *t*-test, P=0.88). (F) COT at U_{burst} was not significantly different between treatments (Student's *t*-test, P=0.69). Box plots show minimum, first quartile, median, third quartile and maximum for each treatment (control in blue, hypoxia in pink). Individual data points are shown (n=6–8 per treatment). *Significant difference between treatments.

Hypoxia-tolerant fish generally display behavioral, morphological and/or physiological plasticity to decrease the consequences of low O_2 exposure. When given the choice, many fish simply avoid hypoxia. For example, red drum display hypoxia avoidance behavior at O_2 levels well above their P_{crit} (Ern and Esbaugh, 2021). To maintain O_2 uptake, fish can remodel their gills to increase surface area and diffusion distance (reviewed by Nilsson et al., 2012) and/or change their blood O_2 binding characteristics (e.g. Mandic et al., 2009). Many fish increase hematocrit (percentage of RBCs in whole blood) and Hb concentration to increase O_2 carrying capacity (e.g. Borowiec et al., 2015; Collins et al., 2016; Petersen and Gamperl, 2011), while some fish increase O_2 binding affinity, measured as a reduced Hb P_{50} (the O_2 tension where Hb is 50% saturated). Hypoxia-acclimated red drum do not show changes in gill morphology (Pan et al., 2017), but Pan et al. (2017) and Negrete et al. (2022), authors of the companion study to this work, demonstrated Hb isoform expression is altered by 8–14 days of hypoxia acclimation and coincides with a decreased Hb P_{50}, increased hematocrit and a significantly lower Root effect (i.e. reduced pH sensitivity). Thus, it appears that red drum exposed to prolonged hypoxia prioritize protecting O_2 uptake at the gill by raising Hb–O_2 affinity, while

sacrificing O_2 extraction via the Root effect by reducing pH sensitivity.

The companion work by Negrete et al. (2022) demonstrated that 8 days of hypoxia acclimation improved organismal aerobic performance in hypoxia, whereby the MMR of hypoxia-acclimated fish was significantly elevated when the fish were tested at 50% O_2 saturation. As the focus of this study was on tissue O_2 extraction, we chose to test the aerobic performance of fish in normoxia, which would reduce the importance of affinity-based traits (i.e. Hb P_{50}) while emphasizing the total capacity for O_2 transport in the cardiorespiratory system. We would expect that if hypoxia acclimation improved O_2 extraction, then MMR would likewise improve. Other studies have shown a slight, but statistically insignificant, increase in MMR in hypoxia-acclimated rainbow trout and Atlantic cod (*Gadus morhua*) when tested in normoxia (Bushnell et al., 1984; Petersen and Gamperl, 2010), and a significant increase in MMR in hypoxia-acclimated goldfish (*Carassius auratus*) when measured under normoxia, due to a modified gill structure and increased blood O_2 binding capacity (Fu et al., 2011). However, we found no significant differences in respiratory performance as a consequence of acclimation. These data generally agree with the biochemical results from the heart and red muscle. However, it is also noteworthy that MMR was not significantly reduced following 8 days of hypoxia acclimation, as the work of Negrete et al. (2022) showed a reduction in the magnitude of the Root effect of approximately 15% at physiological pH and [NTP]. This may suggest that Root effect-mediated O_2 extraction is not a driver of MMR in red drum.

Surprisingly, 8 days of hypoxia acclimation did improve swim performance in red drum. Ackerly et al. (2018) have previously demonstrated that after an 8 week hypoxia acclimation, U_{crit} of the mormyrid *Marcusenius victoriae* was 1.5 times greater than that of control fish when tested under normoxia. Goldfish also improved their U_{crit} after just 48 h of hypoxia acclimation, with ∼18% increase in swim speed under normoxia compared with normoxia-acclimated fish (Fu et al., 2011), although these data coincide with goldfish gill remodeling that is not common to all fishes. Here, we found U_{crit} was significantly higher in hypoxia-acclimated red drum tested in normoxia, despite the fact that there was no significant change in MMR. Interestingly, the average U_{crit} of our 60 g control red drum was within ∼10% of U_{crit} measured in 200 g red drum (Esbaugh et al., 2016), but ∼30% lower than U_{crit} of 20 g red drum (Johansen and Esbaugh, 2017), and ∼62% lower than U_{crit} of 1 g red drum (Khursigara et al., 2021). This may indicate an allometric relationship, wherein red drum U_{crit} decreases with increased body size, as seen in other species (e.g. Bale et al., 2014; Gregory Tolley and Torres, 2002). Note that there were no other differences in swim performance metrics, including COT, U_{opt} and, most importantly, U_{burst}.

Aerobic swim performance is generally considered an important ecological metric, demonstrating the ability of a fish to perform important behaviors such as foraging and predator evasion. While U_{crit} is frequently used as a proxy of aerobic swimming capacity, anaerobic metabolism is also used to reach U_{crit} (Svendsen et al., 2010), and anaerobic capacities may affect U_{crit} in hypoxia-acclimated fish (Cook et al., 2013). U_{burst} indicates the swim speed at which fish begin white muscle recruitment, and thus transition from aerobic swimming to an anaerobically powered burst-and-coast swim gait. While burst swim speed is not significantly different between normoxia- and hypoxia-acclimated red drum, when taken in the context of the swim trial from the predicted onset of white anaerobic muscle recruitment to swim failure, hypoxia-acclimated fish may be utilizing anaerobic metabolism 1.5 times longer than normoxia-acclimated fish (roughly 38 min versus 24 min, respectively). Red drum were acclimated to O_2 levels above their P_{crit}, the O_2 saturation level below which hypoxia-tolerant fish suppress metabolism and shift towards anaerobic energy production (Richards, 2009). Based on our data, we hypothesize that hypoxia acclimation above P_{crit} stimulates plasticity in anaerobic biochemical pathways to elevate non-aerobic sources of energy production given the aerobic constraints of the hypoxic environment. The contribution of anaerobic metabolism to swim performance of hypoxia-acclimated red drum is the most likely underlying mechanism for the observed differences in U_{crit} following hypoxia acclimation, which agrees with the finding that MMR was also not significantly different between acclimated and control fish.

Overall, our results suggest that for red drum, a species that is highly tolerant to and flexible in environmental fluctuations, there are no dramatic changes to tissue O_2 extraction or whole-animal aerobic performance via CA-IV recruitment under hypoxia. Our data indicate that hypoxia acclimation did improve critical swim performance; however, these changes were not driven by enhanced respiratory performance but may instead occur through improved anaerobic contributions during the critical swimming protocol. It is interesting to consider whether the red drum and salmon represent two opposite approaches to balancing the risk and reward of Root effect Hbs, and their implication for performance in hypoxia. Athletic predatory fishes such as salmonids may prioritize maximizing aerobic metabolism by improving O_2 extraction, which also carries a greater risk of deleterious effects of anaerobically driven metabolic acid–base disturbances on Hb function. Conversely, bottom-feeding predators such as red drum may instead prioritize O_2 uptake while reducing the risks of acidosis associated with Root effect Hbs, and augment performance with anaerobic energy sources. As more non-salmonid teleosts are discovered with the characteristics of enhanced tissue O_2 extraction (e.g. Shu et al., 2022), it is increasingly important to consider the functional significance of this system, especially in non-athletic species.

Acknowledgements
The authors would like to thank the anonymous reviewers for their constructive comments, and everyone who kindly assisted with fish care and maintenance: A. Khursigara, J. Lonthair, L. Martin, M. Schumm and A. Zambie.

Competing interests
The authors declare no competing or financial interests.

Author contributions
Conceptualization: A.J.E.; Methodology: A.M.D., B.N., K.L.A.; Validation: A.M.D.; Formal analysis: A.M.D.; Investigation: A.M.D., B.N., K.L.A.; Resources: A.J.E.; Data curation: A.M.D., B.N., K.L.A.; Writing - original draft: A.M.D.; Writing - review & editing: A.M.D., B.N., K.L.A., A.J.E.; Visualization: A.M.D.; Supervision: A.J.E.; Funding acquisition: A.J.E.

Funding
This research was made possible by a grant from the National Science Foundation awarded to A.J.E. (2002549). B.N.J. was supported by National Science Foundation Graduate Research Fellowship Program (1610403), and A.M.D. was supported by the University of Texas at Austin Stengl-Wyer Graduate Fellowship and National Science Foundation Postdoctoral Research Fellowship in Biology (2109765). Any opinions, findings, and conclusions or recommendations expressed in this material are those of the authors and do not necessarily reflect the views of the National Science Foundation.

References

Ackerly, K. L. and Esbaugh, A. J. (2020). The additive effects of oil exposure and hypoxia on aerobic performance in red drum (*Sciaenops ocellatus*). *Sci. Total Environ.* **737**, 140174. doi:10.1016/j.scitotenv.2020.140174

Ackerly, K. L., Krahe, R., Sanford, C. P. and Chapman, L. J. (2018). Effects of hypoxia on swimming and sensing in a weakly electric fish. *J. Exp. Biol.* **221**, jeb172130. doi:10.1242/jeb.172130

Alderman, S. L., Harter, T. S., Wilson, J. M., Supuran, C. T., Farrell, A. P. and Brauner, C. J. (2016). Evidence for a plasma-accessible carbonic anhydrase in the lumen of salmon heart that may enhance oxygen delivery to the myocardium. *J. Exp. Biol.* **219**, 719-724. doi:10.1242/jeb.130443

Allmon, E. B. and Esbaugh, A. J. (2017). Carbon dioxide induced plasticity of branchial acid-base pathways in an estuarine teleost. *Sci. Rep.* **7**, 1-10. doi:10.1038/srep45680

Bale, R., Hao, M., Bhalla, A. P. S. and Patankar, N. A. (2014). Energy efficiency and allometry of movement of swimming and flying animals. *Proc. Natl Acad. Sci. USA* **111**, 7517-7521. doi:10.1073/pnas.1310544111

Bell, W. and Terhune, L. (1970). *Water Tunnel Design for Fisheries Research*. Fisheries Research Board of Canada, Biological Station.

Berenbrink, M., Koldkjær, P., Kepp, O. and Cossins, A. R. (2005). Evolution of oxygen secretion in fishes and the emergence of a complex physiological system. *Science* **307**, 1752-1757. doi:10.1126/science.1107793

Bopp, L., Resplandy, L., Orr, J. C., Doney, S. C., Dunne, J. P., Gehlen, M., Halloran, P., Heinze, C., Ilyina, T., Séférian, R. et al. (2013). Multiple stressors of ocean ecosystems in the 21st century: projections with CMIP5 models. *Biogeosciences* **10**, 6225-6245. doi:10.5194/bg-10-6225-2013

Borowiec, B. G., Darcy, K. L., Gillette, D. M. and Scott, G. R. (2015). Distinct physiological strategies are used to cope with constant hypoxia and intermittent hypoxia in killifish (*Fundulus heteroclitus*). *J. Exp. Biol.* **218**, 1198-1211. doi:10.1242/jeb.114579

Brett, J. R. (1964). The respiratory metabolism and swimming performance of young sockeye salmon. *J. Fish. Board Can.* **21**, 1183-1226. doi:10.1139/f64-103

Bushnell, P. G., Steffensen, J. F. and Johansen, K. (1984). Oxygen consumption and swimming performance in hypoxia-acclimated rainbow trout *Salmo gairdneri*. *J. Exp. Biol.* **113**, 225-235. doi:10.1242/jeb.113.1.225

Claireaux, G., Couturier, C. and Groison, A.-L. (2006). Effect of temperature on maximum swimming speed and cost of transport in juvenile European sea bass (*Dicentrarchus labrax*). *J. Exp. Biol.* **209**, 3420-3428. doi:10.1242/jeb.02346

Collins, G. M., Clark, T. D. and Carton, A. G. (2016). Physiological plasticity v. inter-population variability: understanding drivers of hypoxia tolerance in a tropical estuarine fish. *Mar. Freshw. Res.* **67**, 1575-1582. doi:10.1071/MF15046

Cook, D. G., Iftikar, F. I., Baker, D. W., Hickey, A. J. R. and Herbert, N. A. (2013). Low-O_2 acclimation shifts the hypoxia avoidance behaviour of snapper (*Pagrus auratus*) with only subtle changes in aerobic and anaerobic function. *J. Exp. Biol.* **216**, 369-378. doi:10.1242/jeb.073023

Damsgaard, C., Lauridsen, H., Harter, T. S., Kwan, G. T., Thomsen, J. S., Funder, A. M., Supuran, C. T., Tresguerres, M., Matthews, P. G. and Brauner, C. J. (2020). A novel acidification mechanism for greatly enhanced oxygen supply to the fish retina. *eLife* **9**, e58995. doi:10.7554/eLife.58995

Deutsch, C., Ferrel, A., Seibel, B., Pörtner, H.-O. and Huey, R. B. (2015). Climate change tightens a metabolic constraint on marine habitats. *Science* **348**, 1132-1135. doi:10.1126/science.aaa1605

Deutsch, C., Penn, J. L. and Seibel, B. (2020). Metabolic trait diversity shapes marine biogeography. *Nature* **585**, 557-562. doi:10.1038/s41586-020-2721-y

Diaz, R. J. and Rosenberg, R. (2008). Spreading dead zones and consequences for marine ecosystems. *Science* **321**, 926-929. doi:10.1126/science.1156401

Dichiera, A. M. and Esbaugh, A. J. (2020). Red blood cell carbonic anhydrase mediates oxygen delivery via the Root effect in red drum. *J. Exp. Biol.* **223**, jeb232991. doi:10.1242/jeb.232991

Ern, R. and Esbaugh, A. J. (2016). Hyperventilation and blood acid–base balance in hypercapnia exposed red drum (*Sciaenops ocellatus*). *J. Comp. Physiol. B* **186**, 447-460. doi:10.1007/s00360-016-0971-7

Ern, R. and Esbaugh, A. J. (2021). Assessment of hypoxia avoidance behaviours in a eurythermal fish at two temperatures using a modified shuttlebox system. *J. Fish Biol.* **99**, 264-270. doi:10.1111/jfb.14691

Esbaugh, A. J. and Cutler, B. (2016). Intestinal Na^+, K^+, $2Cl^-$ cotransporter 2 plays a crucial role in hyperosmotic transitions of a euryhaline teleost. *Physiol. Rep.* **4**, e13028. doi:10.14814/phy2.13028

Esbaugh, A. J. and Tufts, B. L. (2006). Tribute to RG Boutilier: evidence of a high activity carbonic anhydrase isozyme in the red blood cells of an ancient vertebrate, the sea lamprey Petromyzon marinus. *J. Exp. Biol.* **209**, 1169-1178. doi:10.1242/jeb.02111

Esbaugh, A. J., Ern, R., Nordi, W. M. and Johnson, A. S. (2016). Respiratory plasticity is insufficient to alleviate blood acid–base disturbances after acclimation to ocean acidification in the estuarine red drum, *Sciaenops ocellatus*. *J. Comp. Physiol. B* **186**, 97-109. doi:10.1007/s00360-015-0940-6

Esbaugh, A. J., Ackerly, K. L., Dichiera, A. M. and Negrete, B., Jr (2021). Is hypoxia vulnerability in fishes a by-product of maximum metabolic rate? *J. Exp. Biol.* **224**, jeb232520. doi:10.1242/jeb.232520

Farrell, A. P. (2007). Tribute to PL Lutz: a message from the heart–why hypoxic bradycardia in fishes? *J. Exp. Biol.* **210**, 1715-1725. doi:10.1242/jeb.02781

Fry, F. (1947). Effects of the environment on animal activity. *Publ. Ontario Fish. Res. Lab.* **68**, 1-62.

Fu, S.-J., Brauner, C. J., Cao, Z.-D., Richards, J. G., Peng, J.-L., Dhillon, R. and Wang, Y.-X. (2011). The effect of acclimation to hypoxia and sustained exercise on subsequent hypoxia tolerance and swimming performance in goldfish (*Carassius auratus*). *J. Exp. Biol.* **214**, 2080-2088. doi:10.1242/jeb.053132

Georgalis, T., Gilmour, K. M., Yorston, J. and Perry, S. F. (2006). Roles of cytosolic and membrane-bound carbonic anhydrase in renal control of acid-base balance in rainbow trout, *Oncorhynchus mykiss*. *Am. J. Physiol. Renal Physiol.* **291**, F407-F421. doi:10.1152/ajprenal.00328.2005

Gregory Tolley, S. and Torres, J. J. (2002). Energetics of swimming in juvenile common snook, *Centropomus undecimalis*. *Environ. Biol. Fishes* **63**, 427-433. doi:10.1023/A:1014938805181

Harter, T. S. and Brauner, C. J. (2020). Teleost red blood cells actively enhance the passive diffusion of oxygen that was discovered by August Krogh. *Comp. Biochem. Physiol. A Mol. Integr. Physiol.* **253**, 110855. doi:10.1016/j.cbpa.2020.110855

Harter, T. S., Zanuzzo, F. S., Supuran, C. T., Gamperl, A. K. and Brauner, C. J. (2019). Functional support for a novel mechanism that enhances tissue oxygen extraction in a teleost fish. *Proc. R. Soc. B* **286**, 20190339. doi:10.1098/rspb.2019.0339

Henry, R. P. (1991). Techniques for measuring carbonic anhydrase activity in vitro. In *The Carbonic Anhydrases*, (ed. S. J. Dodgson R. E. Tashian G. Gros and N. D. Carter), pp. 119-125. Springer.

Henry, R. P., Tufts, B. L. and Boutilier, R. G. (1993). The distribution of carbonic anhydrase type I and II isozymes in lamprey and trout: possible co-evolution with erythrocyte chloride/bicarbonate exchange. *J. Comp. Physiol. B* **163**, 380-388. doi:10.1007/BF00265642

Ito, T., Minobe, S., Long, M. C. and Deutsch, C. (2017). Upper ocean O_2 trends: 1958–2015. *Geophys. Res. Lett.* **44**, 4214-4223. doi:10.1002/2017GL073613

Johansen, J. L. and Esbaugh, A. J. (2017). Sustained impairment of respiratory function and swim performance following acute oil exposure in a coastal marine fish. *Aquatic Toxicol.* **187**, 82-89. doi:10.1016/j.aquatox.2017.04.002

Khursigara, A. J., Rowsey, L. E., Johansen, J. L. and Esbaugh, A. J. (2021). Behavioral changes in a coastal marine fish lead to increased predation risk following oil exposure. *Environ. Sci. Technol.* **55**, 8119-8127. doi:10.1021/acs.est.0c07945

Lonthair, J., Ern, R. and Esbaugh, A. J. (2017). The early life stages of an estuarine fish, the red drum (*Sciaenops ocellatus*), are tolerant to high pCO2. *ICES J. Mar. Sci.* **74**, 1042-1050. doi:10.1093/icesjms/fsw225

Lonthair, J., Dichiera, A. M. and Esbaugh, A. J. (2020). Mechanisms of acid-base regulation following respiratory alkalosis in red drum (*Sciaenops ocellatus*). *Comp. Biochem. Physiol. A Mol. Integr. Physiol.* **250**, 110779. doi:10.1016/j.cbpa.2020.110779

Mandic, M., Todgham, A. E. and Richards, J. G. (2009). Mechanisms and evolution of hypoxia tolerance in fish. *Proc. R. Soc. B* **276**, 735-744. doi:10.1098/rspb.2008.1235

Martin, L. and Esbaugh, A. J. (2021). Osmoregulatory plasticity during hypersaline acclimation in red drum, *Sciaenops ocellatus*. *J. Comp. Physiol. B* **191**, 731-740. doi:10.1007/s00360-021-01356-y

McMillan, O. J. L., Dichiera, A. M., Harter, T. S., Wilson, J. M., Esbaugh, A. J. and Brauner, C. J. (2019). Blood and gill carbonic anhydrase in the context of a chondrichthyan model of CO_2 excretion. *Physiol. Biochem. Zool.* **92**, 554-566. doi:10.1086/705402

Negrete, B., Jr and Esbaugh, A. J. (2019). A methodological evaluation of the determination of critical oxygen threshold in an estuarine teleost. *Biol. Open* **8**, bio045310. doi:10.1242/bio.045310

Nikinmaa, M. (1982). Effects of adrenaline on red cell volume and concentration gradient of protons across the red cell membrane in the rainbow trout, *Salmo gairdneri*. *Mol. Physiol* **2**, 287-297.

Nikinmaa, M., Tiihonen, K. and Paajaste, M. (1990). Adrenergic control of red cell pH in salmonid fish: roles of the sodium/proton exchange, Jacobs-Stewart cycle and membrane potential. *J. Exp. Biol.* **154**, 257-271. doi:10.1242/jeb.154.1.257

Nilsson, G. E., Dymowska, A. and Stecyk, J. A. W. (2012). New insights into the plasticity of gill structure. *Respir. Physiol. Neurobiol.* **184**, 214-222. doi:10.1016/j.resp.2012.07.012

Pan, Y. K., Ern, R. and Esbaugh, A. J. (2016). Hypoxia tolerance decreases with body size in red drum *Sciaenops ocellatus*. *J. Fish Biol.* **89**, 1488-1493. doi:10.1111/jfb.13035

Pan, Y. K., Ern, R., Morrison, P. R., Brauner, C. J. and Esbaugh, A. J. (2017). Acclimation to prolonged hypoxia alters hemoglobin isoform expression and increases hemoglobin oxygen affinity and aerobic performance in a marine fish. *Sci. Rep.* **7**, 7834. doi:10.1038/s41598-017-07696-6

Pelster, B. and Weber, R. (1991). The physiology of the Root effect. In *Advances in Comparative and Environmental Physiology*, vol. 8. Springer. doi:10.1007/978-3-642-75900-0_2

Petersen, L. H. and Gamperl, A. K. (2010). Effect of acute and chronic hypoxia on the swimming performance, metabolic capacity and cardiac function of Atlantic cod (*Gadus morhua*). *J. Exp. Biol.* **213**, 808-819. doi:10.1242/jeb.033746

Petersen, L. H. and Gamperl, A. K. (2011). Cod (*Gadus* morhua) cardiorespiratory physiology and hypoxia tolerance following acclimation to low-oxygen conditions. *Physiol. Biochem. Zool.* **84**, 18-31. doi:10.1086/657286

Pfaffl, M. W. (2001). A new mathematical model for relative quantification in real-time RT–PCR. *Nucleic Acids Res.* **29**, e45-e45. doi:10.1093/nar/29.9.e45

Rabalais, N. N., Turner, R. E. and Wiseman, W. J., Jr. (2002). Gulf of Mexico hypoxia, aka "The dead zone". *Annu. Rev. Ecol. Syst.* **33**, 235-263. doi:10.1146/annurev.ecolsys.33.010802.150513

Rabalais, N. N., Díaz, R. J., Levin, L. A., Turner, R. E., Gilbert, D. and Zhang, J. (2010). Dynamics and distribution of natural and human-caused hypoxia. *Biogeosciences* **7**, 585. doi:10.5194/bg-7-585-2010

Richards, J. G. (2009). Metabolic and molecular responses of fish to hypoxia. *Fish Physiol.* **27**, 443-485. doi:10.1016/S1546-5098(08)00010-1

Root, R. W. (1931). The respiratory function of the blood of marine fishes. *Biol. Bull.* **61**, 427-456. doi:10.2307/1536959

Rummer, J. L. and Brauner, C. J. (2011). Plasma-accessible carbonic anhydrase at the tissue of a teleost fish may greatly enhance oxygen delivery: in vitro evidence in rainbow trout, Oncorhynchus mykiss. *J. Exp. Biol.* **214**, 2319-2328. doi:10.1242/jeb.054049

Rummer, J. L. and Brauner, C. J. (2015). Root effect haemoglobins in fish may greatly enhance general oxygen delivery relative to other vertebrates. *PLoS ONE* **10**, e0139477. doi:10.1371/journal.pone.0139477

Rummer, J. L., McKenzie, D. J., Innocenti, A., Supuran, C. T. and Brauner, C. J. (2013). Root effect hemoglobin may have evolved to enhance general tissue oxygen delivery. *Science* **340**, 1327-1329. doi:10.1126/science.1233692

Salama, A. and Nikinmaa, M. (1988). The adrenergic responses of carp (*Cyprinus carpio*) red cells: effects of P_{O_2} and pH. *J. Exp. Biol.* **136**, 405-416. doi:10.1242/jeb.136.1.405

Shu, J. J., Heuer, R. M., Hannan, K. D., Stieglitz, J. D., Benetti, D. D., Rummer, J. L., Grosell, M. and Brauner, C. J. (2022). Enhanced oxygen unloading in two marine percomorph teleosts. *Comp. Biochem. Physiol. A Mol. Integr. Physiol.* **264**, 111101. doi:10.1016/j.cbpa.2021.111101

Svendsen, J. C., Tudorache, C., Jordan, A. D., Steffensen, J. F., Aarestrup, K. and Domenici, P. (2010). Partition of aerobic and anaerobic swimming costs related to gait transitions in a labriform swimmer. *J. Exp. Biol.* **213**, 2177-2183. doi:10.1242/jeb.041368

Videler, J. J. (1993). *Fish Swimming*. Springer Science & Business Media.

Watson, C. J., Nordi, W. M. and Esbaugh, A. J. (2014). Osmoregulation and branchial plasticity after acute freshwater transfer in red drum, *Sciaenops ocellatus*. *Comp. Biochem. Physiol. A Mol. Integr. Physiol.* **178**, 82-89. doi:10.1016/j.cbpa.2014.08.008

Whitney, P. L. and Briggle, T. V. (1982). Membrane-associated carbonic anhydrase purified from bovine lung. *J. Biol. Chem.* **257**, 12056-12059. doi:10.1016/S0021-9258(18)33676-7

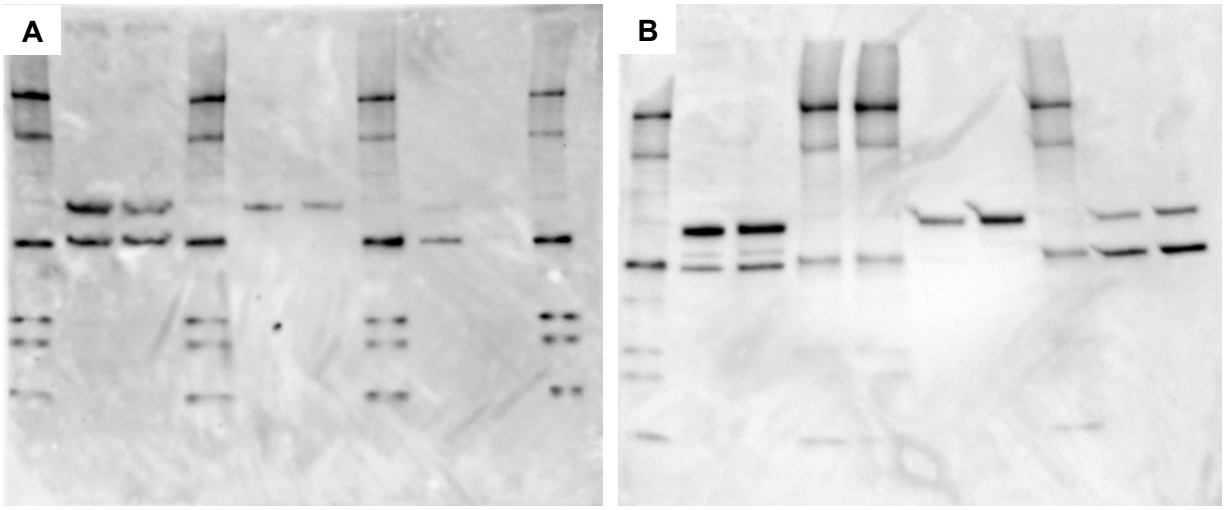

Fig. S1. Primary CA-IV antibody validation using 4-day control and hypoxia heart tissue. Two CA-IV antibodies were tested at 1:1,000 concentration: (A) red drum CA4-1 (B) red drum CA4-2. Red drum CA4-2 was used for the current study. Tissues were processed with RIPA buffer or Mem-PER Plus membrane protein extraction kit. For (A), protein loaded in lanes 2 and 3 were processed using RIPA buffer, protein loaded in lanes 5 and 6 were isolated from the cytoplasmic fraction of the Mem-PER Plus isolation, and protein loaded in lanes 8 and 9 were isolated from the membrane fraction of the Mem-PER Plus isolation. For (B), protein loaded in lanes 2 and 3 were processed using RIPA buffer, protein loaded in lanes 6 and 7 were isolated from the cytoplasmic fraction of the Mem-PER Plus isolation, and lanes 9 and 10 were isolated from the membrane fraction of the Mem-PER Plus isolation. 10 µg of protein was loaded for each sample, and each set of tissues consisted of one control and one hypoxia tissue (e.g., lanes 2 and 3 are control and hypoxia 4-day heart samples, respectively). Precision Plus Protein™ Unstained protein standards (Bio-Rad) were used for the ladders.

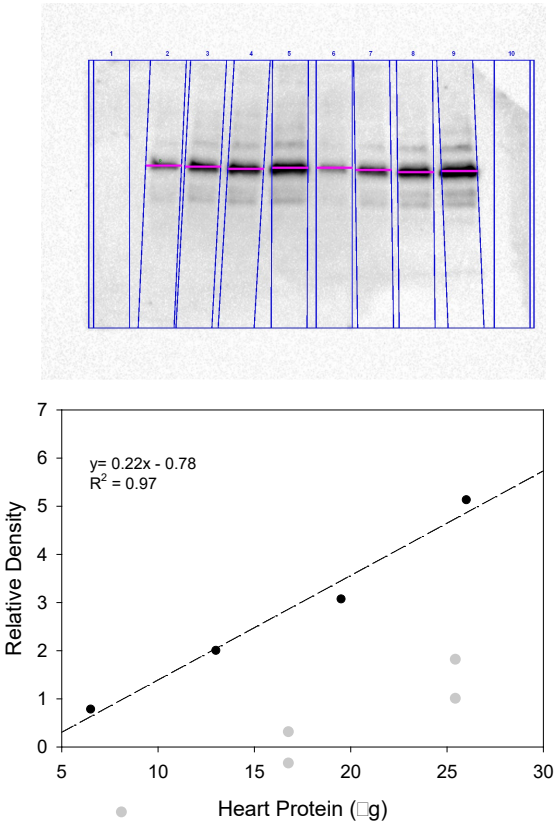

Fig. S2. CA-IV antibody linear response validation using control heart tissue. (A) Western blot demonstrated the linearity of the CA-IV antibody response across a range of heart protein concentrations. Note that in this non-experimental sample the 56 kDa band was dominant relative to the 43 kDa band, and as such the linearity was calculated only relative to this band. (B) The calculated linear function and R^2 based on the relative densities across the loaded total heart protein demonstrated linearity of the CA-IV antibody response in relation to quantity of protein. Black dots represent the mean at each total protein concentration, and gray dots represent the individual data points (n=2 per protein concentration). All bands are calculated relative to the band in lane 2.

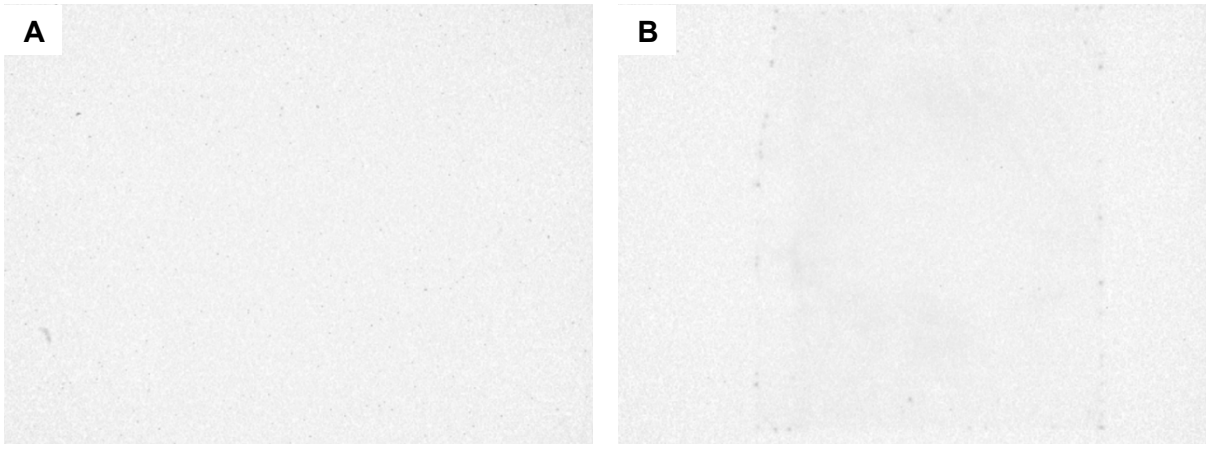

Fig. S3. Primary CA-IV antibody validation using (A) antigen excess and (B) no primary controls. 10 µg of heart protein was loaded for each sample, and each set of tissues consisted of one control and one hypoxia tissue. (A) Antigen excess control consisted of incubating antibody with 10x antigen provided from the manufacturers (GenScript) overnight at 4°C. Western blot protocol was performed as described in Materials and Methods section. No bands were present for either control demonstrating that the primary CA-IV antibody is specific to CA-IV protein and responsible for the bands present in Figure S1.

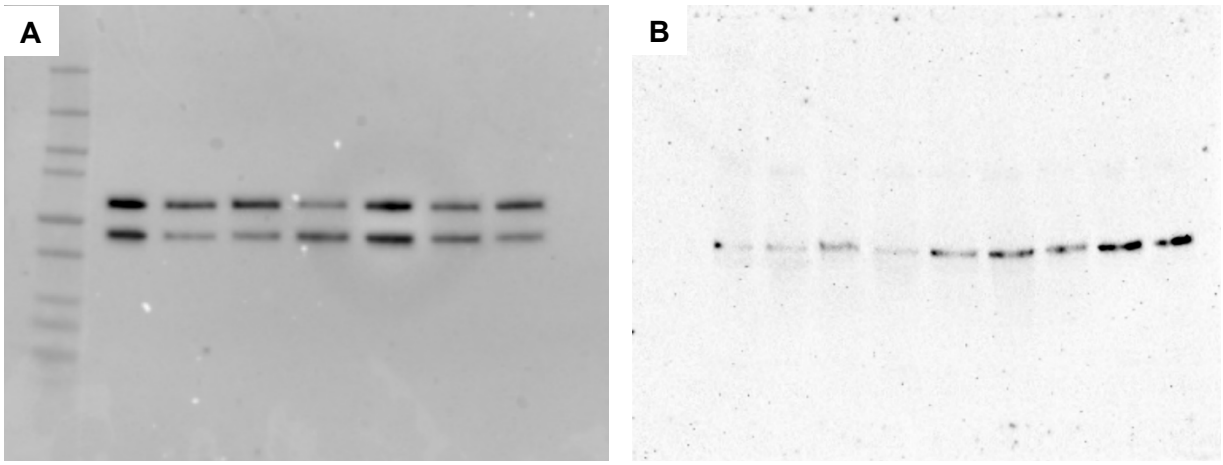

Fig. S4. Representative Western blot images for CA-IV protein at 8 days in the (A) heart and (B) red muscle. (A) A composite image of the Precision Plus Protein™ Dual Color ladder (Bio-Rad) under UV illumination and chemiluminescent image of CA-IV protein demonstrates the weight of each protein band (composite image not used for protein quantification).

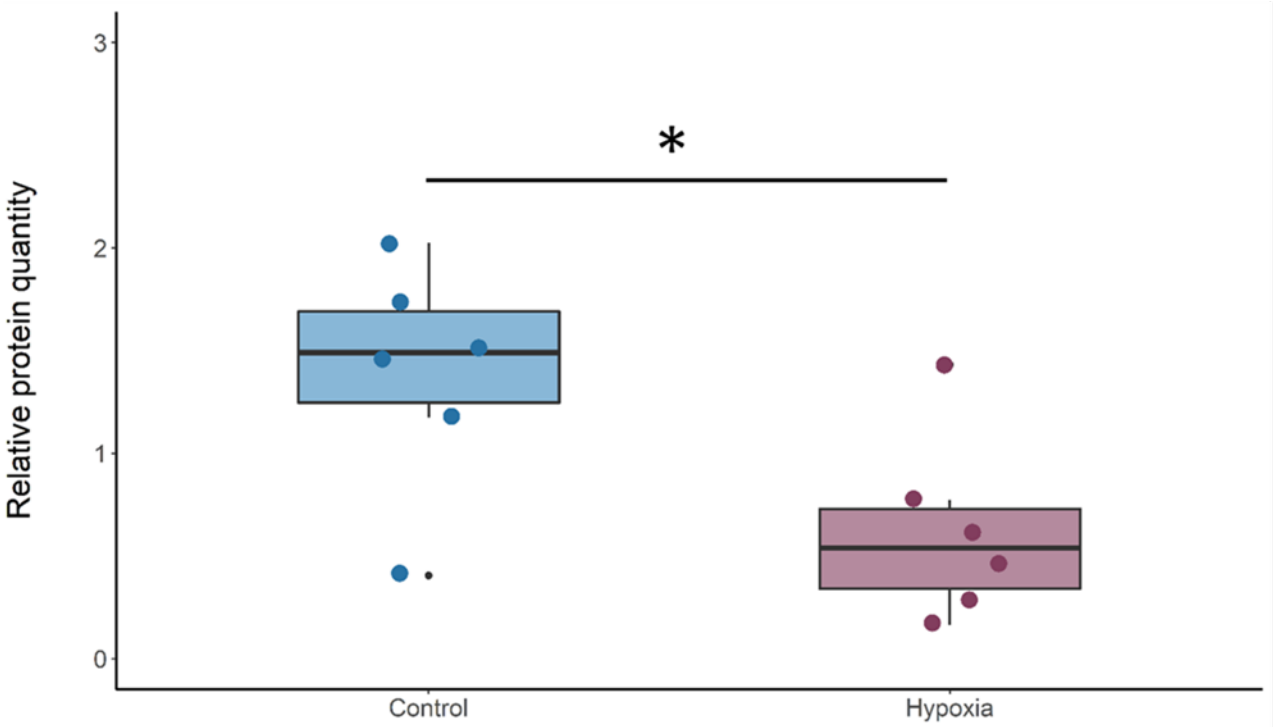

Fig. S5. Comparison of immature CA-IV protein quantity in the heart of red drum acclimated to control seawater or hypoxia for 8 days. There were significant differences in the immature CA-IV protein between treatments for heart (student's t-test, P=0.03). Quantities were calculated relative to a control 8-day (C1A8D) heart sample. Relative quantities were calculated for both for CA-IV protein content and total protein content of each sample. Relative CA-IV protein content was normalized to relative total protein content for each sample to account for any overall reduction in protein due to hypoxia exposure. Therefore, the relative protein quantity of C1A8D is 1. Relative protein quantities were assessed for the 56 kDa band, which we consider the immature form of CA-IV protein. All data are represented as box plots, where the minimum, first quartile, median, third quartile and maximum are presented for each treatment (control presented in blue, hypoxia presented in pink). Asterisk denotes significant difference between treatments. Individual data are overlayed (n=6 per treatment).